BARD

FINAL REPORT

PROJECT NO. US-1573-88

Photometric Imaging for Detecting Surface and Internal Defects on Apples

B.L. Upchurch, D. Aneshansley, J.A. Throop,
R. Ben-Arie, N. Flohr, A. Hetzroni, F. Geoola

1993

40728

DATE: February 11, 1993

BARD
P.O. Box 6
Bet Dagan, ISRAEL

BARD Project No. US-1573-88R

Title

Photometric Imaging for Detecting Surface and Internal Defects of Apples

Investigators' Names	Investigators Institutions
Bruce L. Upchurch	USDA-ARS
Daniel Aneshansley	Cornell University
James A. Throop	Cornell University
Ruth Ben-Arie	Agricultural Research Organization
Nuri't Flohr	Agricultural Research Organization
Amots Hetzroni	Agricultural Research Organization
Farhad Geoola	Agricultural Research Organization

Project's Starting Date: October 1, 1989

Type of Report: 1st Annual _____ 2nd Annual _____ Final X

Bruce L Upchurch
Signature
Bruce L. Upchurch
Principal Investigator

Donald L Peterson, Acting RL.
Signature
D. Michael Glenn, Research Leader
Institution's Authorized Official

Stephen S. Miller
Signature
Stephen S. Miller, Director
Institution's Authorized Official

630.72
SOR/UPC / 634.11
2nd copy

TABLE OF CONTENTS

ABSTRACT

The focus of this research project was to develop a photometric imaging system for detecting bruises on Red Delicious and Golden Delicious apples. As part of the project, an investigation to characterize the physical and chemical alterations that occur when an apple is damaged was undertaken. Project objectives were 1) to characterize the anatomical and chemical changes for bruising, shape, russetting, and external insect damage and how these changes vary with time on Red Delicious, Golden Delicious, and Empire apples, 2) to define the chemical changes for the previously specified apple varieties, and 3) to evaluate the selected photometric sensor and image processing techniques for determining the feasibility of distinguishing good tissue from each defect and each defect-type from each other.

Apple tissue undergoes both chemical and anatomical alterations when cells are damaged. Studies indicated that CO_2 production increased while ethylene production decreased for bruised tissue regions. Membrane permeability increased for bruised tissue and was proportional to the severity of the bruised region. This change in the permeability resulted in an increase in the electrical conductance for bruised apple tissue.

There are limitations of applying spectrophotometric results into a machine vision inspection system. Although specific wavelengths for increasing the contrast between bruised and nonbruised were identified, the contrast between bruised and nonbruised regions actually decreased when the specific wavelengths were implemented in a machine vision system. Bruise detection using near-infrared reflectance varied with time. For a 24 hour bruise, the energy reflected from a bruised region was less than the energy reflected from a nonbruised region. However, the energy reflected from a bruised region exceeded that from a nonbruised site for older bruises. Red, green, and hue were selected as the best features for discriminating bruises on stored Golden Delicious apples. These three features did not exhibit an increase in reflectance for older bruises that was evident with near-infrared reflectance.

Three algorithms for tracing the boundary of pixel clusters were evaluated for their accuracy from measuring the area and efficiency in computation. The CLUSTER and BOUNDARY algorithms were not significantly different in performance or speed, while CENTROID was slowest.

INTRODUCTION

Commercial apple production has increased over the past 25 years despite a decline in the number of acres in production. This continued increase will force the grower to adopt new production practices, because the labor force for harvesting and handling the fruit is declining. Unless the grower can harvest and process the fruit before its quality deteriorates, the fruit will be worthless.

Fruit quality depends on several characteristics that indicate the acceptability of the product to the consumer. For apples, grade is determined by maturity, shape, disease, damage, and color. The complex procedure by which apples are graded is described in the standards adopted by federal government agencies. A satisfactory method for automatically segregating blemished apples is lacking and has led to a labor intensive process for apple inspection. The failure of fully automating apple inspection has led to the following effects on the apple industry in both the United States and Israel:

1. Twenty-five years of mechanized harvesting research has not proved feasible for fresh market apples because of the need for a rapid automated sorting system to remove damaged fruit (Millier et al., 1983, 1984; Tene et al., 1973; Peterson, et al., 1985).

2. Although present technology has automated color and weight sorting, removal of damaged and diseased fruit still remains a labor intensive process.

3. Human failure and fatigue during inspection causes error in equity of payments to producers and variable market quality for the consumer (Rehkugler, 1986). Studies have shown variability in the implementation of the grading standards between packing houses and within a packing house (Stevens and Gale, 1970).

4. Complete sorting of stored apples to eliminate storing damaged fruit that decays and causes spoilage of neighboring good fruit is not fully implemented because the amount of labor necessary to inspect the volume of fruit during the short harvest season cannot be economically justified. However, high speed automatic sorting could make this procedure feasible.

There have been numerous attempts to identify features that could be used to distinguish blemished from unblemished fruit. Many parameters have been identified; however, none have been successfully incorporated into a grading system. Implementation of a successful automatic grading mechanism requires a device that can sense and differentiate many types of fruit characteristics at a high rate of speed and accuracy.

OBJECTIVES

The original objective of this research project was to define a photometric measurement technique for detecting different defects on apples and investigate how these techniques could be applied in a prototype grading system. The specific objectives were:

1. Characterize the anatomical and chemical changes for bruising, shape, russetting, and external insect damage and how these changes vary with time on Red Delicious, Empire, and Golden Delicious apples.

2. Define the relationship between the photometric measurement and the anatomical and chemical changes for the previously specified apple varieties.

3. Evaluate the selected photometric sensor and image processing techniques for determining the feasibility of distinguishing good tissue from each defect type and each defect type from each other.

During the course of the project, the objectives were modified. The type of defects and the cultivars of apples were reduced. Characterization of bruise damage was investigated only on Red Delicious and Golden Delicious apples. This limitation focused the research on the main fresh market cultivars. Quality factors such as shape, russetting, and insect damage were omitted; however, time and storage effects on the dissipation of watercore and development of internal browning were investigated. This change was made, because earlier time studies indicated that the light transmission properties of watercored fruit changed with time and storage conditions. Lacking the input from a postharvest physiologist at the Appalachian Fruit Research Station, no progress was made on evaluating the relationship between the photometric measurement and the anatomical and chemical changes of the various defects.

RESEARCH ACTIVITIES AND RESULTS

Physiological Changes for Alternative Detection

Bruising of apples occurs by compression and impact damage during handling, packaging and transport operations. The result is a loss of prime quality and reduced grades of the fruit on the market. There is an increasing demand to grade fruits for quality and appearance and at present, most of the inspection is done manually. An objective, mechanized technique for produce inspection is needed by the fruit and vegetable sorting, grading and packing industries. Various automatic techniques that have been investigated are based on detection by computer vision using near-infrared (Taylor and Rehkugler, 1985), x-rays (Johnson, 1985), NMR (Chen et al., 1988) and even computer tomography for internal quality (Moroshima et al., 1987). All these methods are aimed at visualizing the defective tissue and thereafter interpreting and translating the vision to a data processing system, which, of necessity has to be very rapid. One of the difficulties with these methods for computer imaging of bruised tissue is, that a bruise generally becomes visible to the naked eye and to the apparatus, some time after the damage has occurred. However, prior to the change in color, a number of physiological and biochemical alterations occur, leading among other things, to the change in color. The object of this study was to characterize some of these changes, with the idea that they might be used as attributes to identify damaged tissue, even at an early stage after its induction.

Selected damage-free fruits of uniform size from two cultivars, Golden Delicious and Starking Delicious were harvested at three stages of maturity. Fruit samples were subjected to measured degrees of impact force, either after

harvest or after various storage periods. The different degrees of impact force were achieved by dropping a 4 cm diameter metal disc, weighing 364 g, from different heights onto the exposed cheek of each fruit. The impact of the disc on the fruit caused a regular circular bruise, the size of which was proportional to the impact force. Physiological responses were monitored at predetermined times immediately following treatment or after cold storage in air or controlled atmosphere (CA: 5% CO_2, 2% O_2). The parameters measured were:

a) Changes in color measured by reflectance from bruised tissue, using a Minolta chromameter CR-200.
b) Respiration and ethylene evolution by whole fruits and from excised bruised tissue compared to excised healthy tissue from the same fruits.
c) Electrolyte leakage from bruised tissue as a measure of membrane damage.
d) Conductivity of bruised tissue compared to healthy areas of the same fruits.
e) Acidity of bruised versus healthy tissue, by titration of extracted juice.
f) Changes in the activity of the ethylene forming enzyme (EFE) in vivo.

a) Bruise detection by tristimulus color measurement

Differential color estimations of bruised vs. healthy tissue (ΔE^*_{ab}), based on Commission International de l'Eclairage (CIE, 1986) L* a* b* (CIELAB) values, correlated well ($R^2 = 0.57$) for green Golden Delicious apples when the total color difference (ΔE^*ab) was calculated as follows:

$$\Delta E^*_{ab} = (\Delta L^*)^2 + (\Delta a^*)^2 + (\Delta b^*)^2$$

As fruit matured, the quantitative color differences diminished, even though the bruises remained visible. A similar situation was observed on bruised fruit that was examined after storage. The above correlation did not hold true for bruises on the red cheeks of Starking Delicious apples.

b) Respiration and ethylene evolution

The respiratory activity and ethylene evolution by whole fruits immediately after impact bruising were essentially the same as reported previously by other investigators (Robitaille and Janick, 1973; Klein, 1983), for both freshly harvested fruits and for post-storage treated fruits (Table 1).

The enhancement of CO_2 production was generally less pronounced with the 2 cvs. studied here, but the inhibition of ethylene evolution was much the same. However, neither respiration rate nor ethylene evolution from stored-bruised fruit showed any consistent significant deviation from those of undamaged fruit, after the removal of the fruit from air or CA storage.

Comparisons drawn between the CO_2 production rates of excised bruised and healthy tissues from the same fruits showed no effect on bruising at any time. Moreover, no differences could be found in the titratable acid content of bruised and healthy tissue. The enhanced malate decarboxylation effect of bruising, proposed by Klein (1983) to explain the increased CO_2 production

Table 1. CO_2 and C_2H_4 production by discs of bruised apple tissue (expressed as % of production by non-bruised tissue discs) excised from fruits at different stages of the climacteric after impact bruising from different heights.

Cultivar	Location	Harvest Date	Impact Ht (cm)	CO_2[a] Pre	CO_2[a] C1	CO_2[a] Post	C_2H_4[a] Pre	C_2H_4[a] C1	C_2H_4[a] Post
Golden Delicious	Valley	28/8/90	10	114	71		-	61*	37*
			15	115	119		-	48*	-
			20	122	113	86	-	40*	28*
		11/9/90	10	111	121	71	52	52*	32*
			15	128	92	-	77	35*	-
			20	106	104	79	30*	32*	37*
		18/9/90	10	-	89	93	-	65*	35*
			20	-	111	95	-	38*	33
Starking Delicious	Plateau	2/20/90	10	-	125	89	-	69*	77
			20	-	97	95	-	59*	62

a - Production 4h after impact
Pre - preclimacteric fruit
C1 - at climacteric peak
Post - postclimacteric fruit
*Differs from control at p=0.05

from damaged fruits, does not appear to apply for Golden Delicious apples. This might be due to the low level of acidity in Golden Delicious as compared to McIntosh. It would therefore seem that increased CO_2 production does not necessarily accompany bruising of apples.

On the other hand, when comparisons were drawn with regard to ethylene evolution, consistent inhibition was observed for at least 6 hours after impact. The extent of inhibition was relative to the severity of the bruise at 2 hours after impact, but the differences diminished somewhat thereafter. At 24 hours after excision, when wound ethylene was no longer being produced, only the more severely bruised tissue produced ethylene at a lower rate than that of the healthy tissue. Even though the ethylene produced by intact stored-bruised fruit did not appear to have been affected by prestorage bruising, production by excised bruised tissue was reduced relative to that of excised healthy tissue from the same fruits (i.e. with respect to ethylene evolution, stored-bruised tissue behaved in a similar manner to freshly bruised tissue). Measurement of EFE activity indicated that a decline in the ability of this enzyme to catalyze the formation of ethylene from aminocyclopropane-1-carboxylic acid (ACC), is likely to be the cause of reduced ethylene production in bruised tissue.

c) Membrane permeability

Membrane permeability changed with fruit maturation; however, bruising increased the amount of electrolytes leaking out of the tissue plugs. The maximum response to bruising took longer to develop than either change in color or reduction in ethylene evolution, and was achieved at about 90 minutes after bruising. The effect of bruising on membrane permeability was not reversible and could be measured to a similar extent in bruised-stored fruits and under all conditions of impact. The extent of leakage was in proportion to the severity of the bruise and to the force of impact. Leakage from lightly bruised tissue, achieved with the lowest impact force used, was not always significantly higher than that from the healthy tissue of the same fruits.

d) Tissue conductivity

The consistent effect of bruising on electrolyte leakage from damaged tissues compared to healthy tissue from the same fruits, led us to try to measure this difference in intact fruits. The use of a conductivity bridge and 2 syringe needles to serve as electrodes, enabled us to monitor significant differences in the conductivity of bruised and healthy tissues. The conductivity of the bruised tissue increased rapidly relative to that of the surrounding healthy tissue, within 30 minutes after impact, and in proportion to the force of impact (R=0.84). This was true for all fruit examined within 24 hours after bruising and the difference tended to increase as the fruit ripened and senesced (i.e. became more susceptible) (Klein, 1987).

Since the above method requires penetration of the fruit surface, attempts were made to develop a nondestructive technique for detecting the changes in internal conductivity by monitoring differences in conductivity around the fruit surface. Unfortunately, the use of primitive equipment prevented the collection of conclusive data. It is still possible that with more sophisticated equipment meaningful data could be obtained.

Of the four physiological parameters found to change in bruised apple tissue, electrical conductivity appeared to be the most reliably consistent and highly correlated with bruise severity. Moreover, it was rapidly detectable and long lasting. The difficulty remains of finding a suitable method for detecting the signal nondestructively. In all events, detection of real differences will require direct contact between a suitable probe and the entire fruit surface. Therefore, it might not be a very practical solution without an ingenious idea of how it can be implemented.

Spectrophotometric Characteristics of Bruised Tissue

Numerous attempts have been made to identify the destructive and nondestructive methods that could be used to distinguish between bruised and nonbruised surface tissue on apples. Brown et al. (1974) and Reid (1976) demonstrated that freshly bruised tissue has a lower reflectance than nonbruised tissue in the visible through near-infrared. Bilanski at al. (1984) and Pen et al. (1985) reported specific wavelengths for distinguishing between the bruised and nonbruised tissue on peeled apples. The wavelengths of their studies ranged from 350 nm to 750 nm. Upchurch et al. (1990) investigated the diffuse reflectance in the 400 to 1000 nm wavelength region

for bruised and nonbruised areas on whole Red Delicious apples. From the reflectance spectra data, different models were developed, and wavelengths most related to bruised areas were identified for each model by linear regression analysis. Only 2.5 - 3.5% of the fruit misclassified resulted from this study.

This project was devoted to study the spectrophotometric characteristics of bruised surface tissue on Golden Delicious apples, in the range of 400 to 840 nm, as a first step toward the development of a nondestructive method for detection of fresh surface bruises caused by impact. The specific objective was to define a classifier that uses the diffuse light reflectivity characteristics at one or more pre-defined narrowbands in the spectrum.

Apples were harvested from different growing regions in Israel and stored at 0° C in air. The apples used for each set of experiments were from the same harvest. Experiments were conducted with apples from air storage (stored apples) at different times of the year, so that the used apples were from 1 to 6 months old. A series of experiments were also conducted with fresh (nonstored) apples during the harvesting seasons. Prior to each experiment, a certain number of apples were removed randomly from storage and allowed to equilibrate at room temperature for 1 hour. The apples for the experiment were randomly selected and bruised by a device identical to the one designed and used by Upchurch et al. (1990). The device consisted of a transparent open ended PVC tube of 4 cm diameter and 35.6 cm height containing a plunger with a 3.9 cm diameter steel disk, weighing 364 g.

Diffuse reflectance of surface tissue of bruised and nonbruised apples was measured using a Philips PU-8000 double beam scanning computerized spectrophotometer equipped with an integrating sphere. The wavelength resolution was 2 nm. The spectrophotometer was calibrated using a standard white sample of known spectrum for 100% reflectance. In the initial stage, reflectivity values of the surface tissue in the range of 400 to 840 nm were obtained for 100 nonbruised stored apples, 100 stored apples that were bruised and maintained at room temperature for 24 hours, and 100 stored apples that were bruised and maintained at room temperature for 90 minutes. In all of the reflectivity measurements, the cheek of interest was sliced appropriately since the sample compartment of the spectrophotometer could not contain a whole apple. The sliced pieces with a minimum thickness of 15 mm, at the target area, were then easily placed against the objective aperture of the integrating sphere. It has to be mentioned that maintaining bruised apples at room temperature allowed for bruise development, thus affecting the reflection of surface tissue. The error of classification of the selected model and selected waveband were tested on a prediction set consisting of 200 stored apples (100 bruised and 100 nonbruised) and 200 fresh nonstored apples (100 bruised and 100 nonbruised).

For each set of experiments an average reflectivity spectra was obtained. The maximum, minimum, and average reflectance spectra of nonbruised and bruised surface tissue after 90 minutes and 24 hours are shown in Figures 1 and 2, respectively. Comparing the spectra in Figure 1, bruised apples which were maintained for 90 minutes after impact reflected less of the radiation between 400 and 800 nn than nonbruised apples. The amount of reflected energy from tissue of bruised apples which were maintained for 24 hours after impact (Fig. 2), was less between 400 and 600 nm when compared to nonbruised apples.

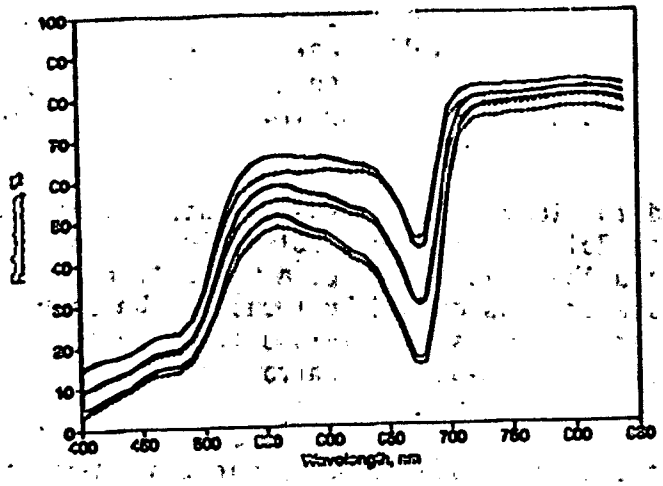

Figure 1. Average, minimum, and maximum reflectance spectra from the surface of Golden Delicious apples after 24 hours.

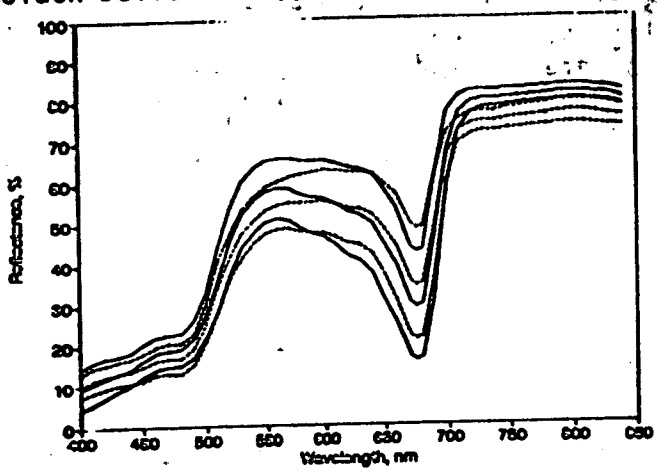

Figure 2. Average, minimum, and maximum reflectance spectra from the surface of Golden Delicious apples after 90 minutes.

However, reflected energy in the 600 to 700 nm region from bruised apples exceeded the corresponding values of the nonbruised apples. From wavelengths 700 nm up to 840 nm, the reflectivity values of the nonbruised surface tissue exceeded the corresponding values of the bruised surface tissues.

The next step toward accomplishing the main objective of the project was to develop a classification criteria by which the bruised and nonbruised surface tissues could be distinguished. In the present study a relation of the following type was considered:

$$M = f(r_{\lambda i}) \qquad (1)$$

In equation (1), $r_{\lambda i}$ represented the reflectance value at a wavelength λi, where i indicates the discrete wavelength involved in computation of the value of M (note that i does not represent a sequential order). Most of the models tested in this study were presented earlier by Upchurch et al. (1990). The models were:

$$M = r_{\lambda i} \quad (2)$$

$$M = \left(\sum_{i=1}^{n} r_{\lambda i}\right)/i \quad (3)$$

$$M = r_{\lambda 1}/r_{\lambda 2} \quad (4)$$

$$M = r_{\lambda 1} - r_{\lambda 2} \quad (5)$$

$$M = (r_{\lambda 1} - r_{\lambda 2})/r_{\lambda 3} \text{ or } r_{\lambda 1}/(r_{\lambda 2} - r_{\lambda 3}) \quad (6)$$

$$M = (r_{\lambda 1} - r_{\lambda 2})/r_{\lambda 3} - r_{\lambda 4}) \quad (7)$$

$$M = (r_{\lambda 1} - r_{\lambda 2})/(\lambda 1 - \lambda 2) \quad (8)$$

In equation (8), M represents the slope of the connecting line between two selected points. In addition to the above equations, a few biased models with different weighting factors were tried which were unsuccessful. The above models were studied and tested on the basis of the reflectance spectra data of nonbruised tissue. In other words, the developed model predicted a nonbruised tissue. Each model after its development (i.e. once the values of λi were determined) was applied to the data of bruised apples, to check the validity of the model for bruise detection.

In general the models involving subtraction of reflectivity values, (i.e. models 5 through 8 are reasonable choices when the differences are large enough to cover the unpredicted measurement errors. Each of the above models was studied and tested in selected narrow wavebands in the range of 400 to 840 nm; however, wavelengths between 400 to 720 nm were not selected for reliable bruise detection purposes.

Formal comparison of models (2) and (3) indicated that model (2) was much simpler to use since it involved the magnitude of reflectance at a single wavelength. However, due to unexpected sources of errors, fluctuation in the magnitude of the reflection data, and identifying a single reflectance wavelength, models based on a single term were subject to large classification errors. Therefore, model (3) was selected as the mathematical model of bruise detection. Further experiments with the existing data also revealed that wavelengths of interest could be reduced from 720 - 840 nm and 750 - 800 nm when using the ratio as the model of bruise detection. The average reflectance in the waveband 750 to 800 nm for the nonbruised apples was found to be 80.74% with a standard deviation of 0.93. For 95% confidence limit the lower band reflection for acceptance of nonbruised apple was found to be 78.88%. On the basis of the present data at this stage, it was concluded that an apple could be classified as nonbruised if $\bar{r} \geq 78.88\%$ and classified as bruised if $\bar{r} < 78.88\%$ where $\bar{r}$ represents the average reflectance of surface tissue of a Golden Delicious apples in the range 750 to 800 nm. To examine the validity of the selected waveband and classifying model, 300 stored apples of which 100 were nonbruised, 100 bruised and kept for 90 minutes at room temperature and 100 bruised and set for 24 hours at room temperature were examined. The result of classification of the experiment is shown in Tables 2 and 3.

Table 2. Results for the ratio model when applied to 300 apples from storage

Percent (%) Correctly Classified	
Nonbruised	Bruised
96.1	88.4 (after 90 min.) 98.7 (after 24 hours)

Table 3. Results of the ratio model when used to classify bruised tissue on nonstored apples.

Percent (%) Correctly Classified	
Nonbruised	Bruised
92.9	91.8

Development of a relatively quick spectrophotometric method of bruise detection of Golden Delicious apples was the main objective of this study. Average reflectance in the wavelength ranging from 750 to 800 nm produced the best criteria for classification of Golden Delicious apples for bruise detection. Application of the method showed misclassification errors of 3.9%, 11.6% and 6.0% for nonbruised, bruised (90 minutes) and bruised (24 hours) stored apples, respectively. This method was also applied to fresh nonstored apples which resulted in misclassification errors of 7.1% with nonbruised and 8.2% with bruised apples.

Spectrophotometric Results and Machine Vision.

Past research on automatic bruise detection on apples has emphasized differences in the near-infrared reflectance between bruised and nonbruised tissues. Utilizing advances in computer vision technology in conjunction with near-infrared reflectance, identification of bruised regions on apples has been attempted with matrix as well as line scan cameras (Graf et al., 1981; Taylor et al., 1984; Rehkugler and Throop, 1986, 1987; Davenel et al., 1988). Earlier spectrophotometric studies had shown that bruised apple tissue had a lower reflectance in the visible through near-infrared region (Brown et al., 1974). Later studies had identified specific wavelengths in the near-infrared region that could be used to enhance the difference between bruised and nonbruised regions on nonpeeled apples (Upchurch et al., 1990). In the study by Upchurch et al. (1990), the ratio between the reflectance at 780 and 830 nm resulted in a misclassification error of less than 5% on nonpeeled Red Delicious apples. However, there has been no attempt to implement and test these wavelengths in a machine vision system. The objective of this project was to evaluate the effectiveness of narrow band filters in a machine vision system for enhancing the contrast between the bruised and nonbruised regions on Red Delicious apples.

A sample of 85 Red Delicious apples were hand harvested and stored in conventional cold storage (0° C). Each apple was bruised by dropping a 39 mm

steel disk a distance of 200 mm onto the surface of the fruit. Prior to capturing an image, the apples were held at room temperature for 24 hours to allow for bruise development. Apples were individually rotated before a line scan camera in a diffusely illuminated chamber (Taylor,1985). Images were captured at each wavelength band. Filters used in front of the camera were a 780 nm with a 11 nm bandwidth, 830 nm with a 12 nm bandwidth, and a long pass near-infrared filter. An image size of 64 pixels (row) by 240 pixels was acquired. Algorithms were written to align the images so that a final image could be generated by a pixel-pixel division between the 780 and 830 images. A mean gray-level within a 15 by 15 pixel window was used as a measure of the reflectance from bruised and nonbruised regions on individual apples.

The contrast improvements for the four different filtered images are shown in Figure 3. Each profile is a plot of the gray-levels for a single row of pixels that bisected a bruised region on an apple. From this sequence, the reflectance difference between bruised and nonbruised regions was greatest in the 780 and long pass near-infrared images. Ratioing the 780 and 830 images actually reduced the difference between bruised and nonbruised regions without reducing the pixel-to-pixel variations in the image. A comparison of the mean gray-level for the two regions exhibited similar results (Table 4). The

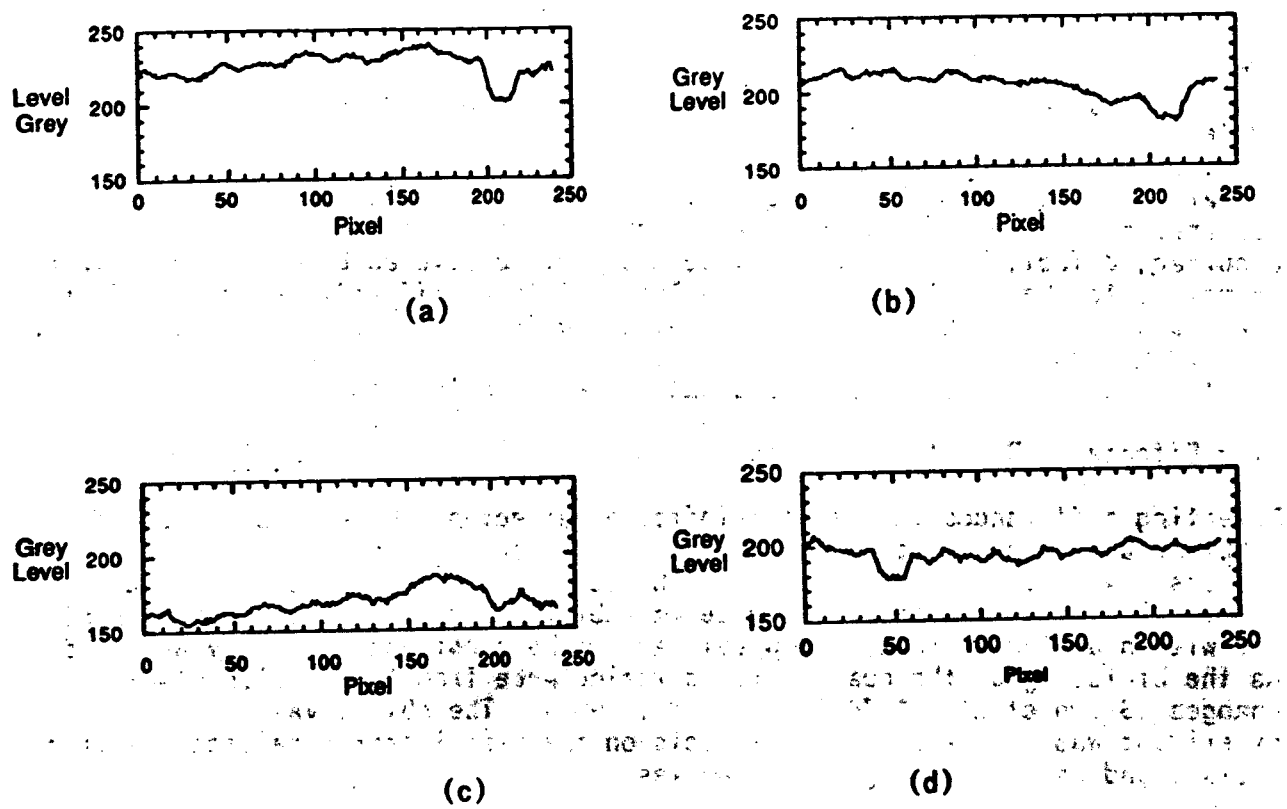

Figure 3. Gray level profile of a single row of Pixels that bisected the bruised region at a) 789 nm, b) 830 nm, c) ratio 780/830, and d) NIR Long Pass.

broadband near-infrared image yielded the best contrast between bruised and nonbruised regions. Assuming a normal distribution of the means, the broadband misclassified 18.7% of the nonbruised regions and 14.4% of the bruised ones. The errors occurring with the 780 image were comparable to the broadband images. However, there was a significant difference in errors in both the 830 and ratio images. Both sets of images had errors in excess of 25%.

Table 4. Probability of incorrectly classifying bruised and nonbruised regions in an apple image.

Image Type	Misclassification (%) Bruised as Nonbruised	Nonbruised as Bruised
780	20.9	19.1
830	34.9	26.3
NIR	18.7	14.4
Ratio	33.4	33.8

Although Upchurch et al. (1990) showed that the ratio improved bruise detectability, contradicting results were found when the fiber optic detector was replaced with a camera and lense system. The bruise was evident in the 830 nm image while 830 nm in the spectrophotometric study was not highly correlated with bruised regions.

Several possible factors could contribute to the lack of success in implementing the spectral information into a machine vision system. First, a difference in precision existed between the two instrumentation systems. The spectrophotometer had the capability to measure smaller changes in reflectance compared to the machine vision system. Another factor is nonlinearity response of the solid-state camera. Finally, the bruise cannot be considered a surface defect, but is a subsurface one that is covered by an infinite thick (compared to the wavelength) layer. The peel is a diffusely reflecting layer that masks part of the energy being reflected from the bruised tissue. In the spectrophotometer, the light source and detector were arranged so that the light energy from the apple tissue was the main reflection.

Time Effects on Detecting Bruises.

Detecting differences in the near-infrared reflectance between bruised and nonbruised regions on apples has had limited success with machine vision systems. As shown by previous research, automatic bruise detection is a difficult problem caused by the wide variability in reflectance between apples and within a single fruit. Temporal factors have not been formally analyzed. As the bruise ages, the near-infrared reflectance from that region also changes (Brown et al., 1974;Graf et al., 1981). The objective of this experiment was to evaluate time effects on the near-infrared reflectance from bruised and nonbruised regions on apples.

Red Delicious and Golden Delicious apples were hand harvested in mid-September during the 1991 season. A total of 64 fruit for each variety were placed in tray packs and stored in conventional cold storage at 0°C. Prior to the first

inspection date, each fruit was bruised by dropping a 39 mm diameter steel disk from a distance of 200 mm onto the surface of the fruit. Samples were held at room temperature, 20°C, for 24 hours to allow for the damaged area to develop the browning that is indicative of bruise damage. For each sampling date, fruit were removed from storage 24 hours prior to inspection. Images of each apple were acquired at one month intervals for two months beginning in November.

Images of apples were acquired by digitizing the output from a RS-170 solid-state camera. A PC-based system equipped with a Data Translation frame grabber and frame processor was used to acquire the images. Images were transferred to a VAX 4000/200 (Digital Equipment Corp.) and analyzed with image processing software from Euclid Computer Co. A CCD array camera (Model 4810, COHU Electronics) without the infrared blocking filter was used to acquire images of the apples. A 25mm lense with an aperature set at f1.4 was mounted to the camera. To limit the reflectance from the apple to the near-infrared region, a long pass filter (Kodak Wratten 89B) was placed between the camera lense and apple. Two images of each apple were captured. The bruised region was centered in the initial image while a second image was acquired after rotating the apple 135° so that the bruised region was absent in the image. To maintain equivalent measurements between dates, a reference image of a teflon cylinder was acquired at four times on each date.

The mean value of the pixels around a circular profile at 1° increments was a measure of the intensity of near-infrared reflectance (NIR) from bruised and nonbruised regions. Three concentric circles were used (Figure 4).

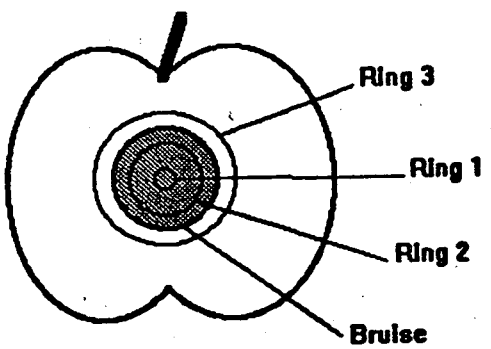

Figure 4. Diagram showing the location of the 3 concentric profiles on the apple.

Initially, the center of the bruised region was interactively identified in the image and used as the center for the concentric profiles. To determine the diameter of the outer two circles, the outer edge of the bruised region in the y-direction was measured interactively. The diameter of the middle profile was twice the difference between the center and outer location minus 30 pixels while the outer circle had a diameter twice the difference plus 30 pixels. The third circular profile had a constant diameter of 10. After measuring the mean gray value around each circle, the three profiles were applied to the nonbruised side. Each mean value was divided by the mean for the reference and then multiplied by 255. Since the relative changes in reflectance between bruised and nonbruised regions were important, the

difference between adjacent profiles (nonbruised - bruised) were calculated and compared. This procedure was repeated on the nonblemished side by calculating differences between nonbruised regions.

Time had a significant effect of the near-infrared reflectance from bruised and nonbruised regions on both Red Delicious and Golden Delicious apples. Comparing a linear profile that disected a bruised region, the reflectance from a bruised region decreased to minimum level with time (Figure 5).

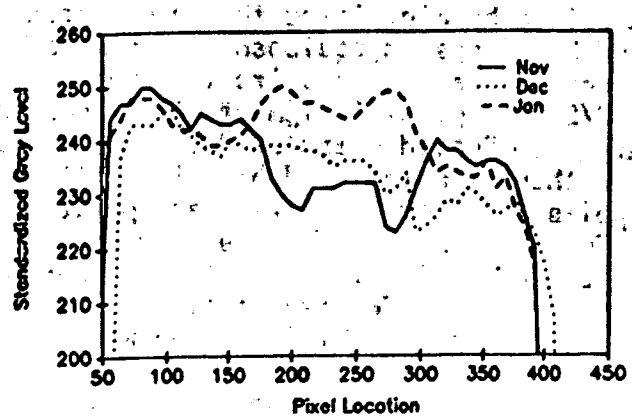

Figure 5. Linear profiles showing the pixel intensities across the apple and how the reflection from a bruised region changes with time.

The maximum difference in reflectance usually occurred 24 hours after inducing the bruise. After one month in storage, the reflectance from the bruised regions increased to a level equivalent to the reflectance from nonbruised regions. This increase in reflectance continued until the reflectance from bruised regions exceeded that from nonbruised regions. Reflectances from Golden Delicious exhibited similar changes with time. The two profiles from the bruised regions on Red Delicious and Golden Delicious apples were significantly different ($Pr < 0.05$) from the nonbruised regions for the 24 hour test (Tables 5 and 6).

Table 5. Effects of time on the reflectance from bruised and nonbruised regions on Red Delicious apples as measured by the mean gray-level of a circular profile.

Profile Size	TEST DATE Nov Mean	Nov Std	Dec Mean	Dec Std	Jan Mean	Jan Std
BRUISED SIDE						
small	231[a]	8.0	235[a]	6.5	244[a]	4.1
medium	230[a]	8.4	235[a]	7.3	247[b]	3.8
large	241[b]	7.6	238[a]	5.0	242[a]	3.7
NONBRUISED SIDE						
small	244[b]	7.5	242[a]	5.0	244[a]	4.9
medium	243[b]	7.5	241[a]	5.1	244[a]	4.5
large	242[b]	7.5	239[a]	4.8	243[a]	4.4

*Means with the same letter are not significantly different at 95% confidence level.

Table 6. Effects of time on the reflectance from bruised and nonbruised regions on 'Golden Delicious' apples as measured by the mean gray-level of a circular profile.

Profile Size	TEST DATE Nov Mean	Nov Std	Dec Mean	Dec Std	Jan Mean	Jan Std
BRUISED SIDE						
small	238[c]	5.5	244[b]	3.1	244[a]	7.4
medium	237[c]	4.8	246[a]	2.8	244[a]	7.2
large	246[b]	4.4	236[a]	3.1	244[a]	7.4
NONBRUISED SIDE						
small	247[a]	5.0	244[b]	3.3	243[a]	7.6
medium	246[b]	4.6	244[b]	3.1	242[a]	7.5
large	249[b]	5.4	245[a]	3.4	243[a]	7.8

*Means with the same letter are not significantly different at the 95% confidence level.

For both varieties, there were no significant differences between the four nonbruised profiles. After one month in storage, the mean reflectance from bruised regions increased to a level where there were no significant differences between any profiles. A significant difference only existed for the middle profile from the bruised region for the third test date on Red Delicious (Table 5). However, there were no significant differences between the profiles on Golden Delicious for the final date (Table 6).

Automatic bruise detection by machine vision depends upon the ability of the system to detect spatial and magnitude relationships between groups of pixels. The maximum difference in reflectance between bruised and nonbruised areas was 16 gray levels which is approximately a 10-15% decrease in reflectance (Figure 6).

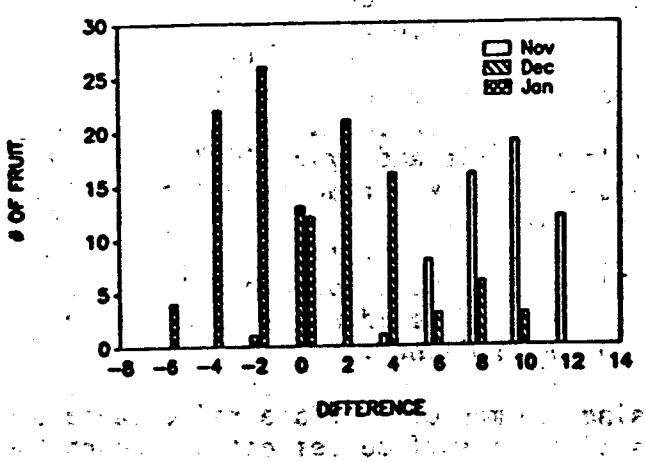

Figure 6. Distribution of the differences between the larger two profiles on the bruised side of the fruit. A negative difference indicated that the reflectance from the bruised region was greater than that from the adjacent nonbruised site.

This maximum difference occurred between the larger two profiles on the bruised side. For the 64 Red Delicious apples, the mean difference was initially 11.3. This mean difference decreased to 3.5 in December and -4.5 in January. A negative difference indicated that the reflectance from the bruised region was greater than the adjacent nonbruised site. Mean differences among the nonbruised regions were within 2 gray levels for the three test dates.

Near-infrared reflectance from bruised regions on Red Delicious and Golden Delicious apples changed with time while the reflectance from nonbruised regions remained relatively constant. This change in reflectance is critical when machine visions systems are being designed to automatically detect bruises on apples. An automatic bruise detection system must be able to detect bruises of various ages. However, the detection is more difficult when the amount of light reflected from the bruised area varies with time.

Color Image Processing of Golden Delicious Apples.

The appearance of Golden Delicious apples is the primary factor on which the consumer makes a purchasing decision. The consumer expects bruise and blemish free fruit. The eye is a sensitive sensor that uses spectral reflectance from the apple surface to judge overall quality. As the technology became available, it was only natural for scientists to measure surface reflectance to quantify apple quality and maturity.

Mechanical injury of Golden Delicious apples can result in softening and discoloration of the tissue under the apple's skin. The discoloration or browning of fruits is ascribed to the oxidation and polymerization of phenolic compounds (Walker, 1964). Unlike red cultivars which tend to mask the browning, the partially translucent yellow skin of Golden Delicious apples allows the browning to show through the skin in sharp contrast to the uniform fruit color. Spectral reflectance at 600nm was used to measure browning on Golden Delicious apples and was correlated with time and temperature (Ingle and Hyde, 1968) Discoloration was expressed as the difference between normal and injured tissue reflectance. Golden Delicious were found to discolor erratically and more slowly than other cultivars and temperature was found to have little effect on the rate of browning (Ingle and Hyde,1968). The reduction in surface reflectance between normal and bruised tissue for Golden Delicious was found to be about 8% compared to 11% for red cultivars such as Red Delicious and McIntosh (Ingle and Hyde, 1968). Surface reflectance using wavelengths between 700 - 2200nm was reduced for bruised compared to normal Golden Delicious tissue (Brown et al., 1974). The significance of this finding was that it removed color variations from the reflectance measurement for bruised tissue. All of the above surface reflectance measurements were made with spectrophotometers and would not be applicable to high speed measurement required on packing lines.

Digital image processing can measure surface reflectance over the total fruit surface to find areas of lower surface reflectance which could be bruises. This method has the potential to measure surface reflectance of a stream of apples on the packing line. Linear discriminate classifiers were determined from a training set of apples with known bruise areas (Graf,1982). Predicting bruised tissue on Golden Delicious apples, NIR reflectance for wavelengths between 750nm to 850nm showed correlations to actual bruising of 0.22 compared

to 0.72 or better for Delicious and McIntosh (Graf,1982). When the apples were cut after testing, a layer of good tissue cells was found just under the skin of the Golden Delicious, unlike Delicious and McIntosh which had damaged cells (Graf, 1982). This observed reduction in surface reflectance in both the visible and NIR wavelengths for bruised tissue on Golden Delicious apples leads to the objectives of this study to examine digital imaging of diffuse surface reflectance in the visible and NIR spectrums as methods for detecting bruises on Golden Delicious apples and determine which features of reflected light (NIR,RGB, and HSI) are the most effective for detecting damaged tissue on Golden Delicious apples before and after storage.

A group of 88 Golden Delicious apples were hand harvested in mid-September during the 1991 harvest season at the Appalachian Fruit Research Station in Kearneysville, WV. A 39 mm diameter steel disk was dropped onto the surface of each fruit. Samples were held for 24 hours at 20°C to allow full bruise development and then digital images were captured (time 1). Thereafter, images were grabbed twice at one month intervals (time 2 and time 3). The apples were removed from cold storage 24 hours prior to imaging and held at 20°C. Two 512 pixel x 512 pixel images (NIR and RGB) of every apple were acquired; one with the bruise normal to the lense and a second with the bruise rotated 105 degrees away from the lense axis displaying only undamaged tissue. Image processing of all images consisted of interactively locating and recording the location of the center of the bruised area as described in previous section.

Surface reflectance of nonbruised tissue for Golden Delicious was found to decrease significantly from the fruit center outwards for the reflectance features of NIR, red, green, blue, hue, and intensity ($p<0.01$). However, saturation exhibited a significant ($p<0.01$) increase. A color difference for good tissue was found between ring 3 that was outside the bruised region and ring 3 from the nonbruised side. There was less red, more green, more blue, greater hue, less saturation and more intensity on the nonbruised side of the apples versus the bruised side ($p<0.01$). From the data collected it was not possible to tell if this difference was an interaction from the bruising process in good tissue adjacent to bruised tissue or was a natural color variation. NIR, green, red and hue (Figure 5a) were more effective for discriminating bruised from nonbruised areas (largest t-values for comparison of rings 2 and 3 at the bruise location). Large variations in surface reflectance for blue, saturation, and intensity reduced their discriminating ability (Figure 7b). Red, green and hue (Figure 8b-d), unlike NIR (Figure 8a), did not show the increase in reflectance for bruised tissue with storage time. These features could be used to form a discriminate function for identifying bruising on stored Golden Delicious apples.

Cluster Segmentation - Evaluation of Algorithms.

In recent years, image processing for agricultural applications has been widely used in research and industry. Many of these algorithms trace the boundary of pixel clusters and determine their area.

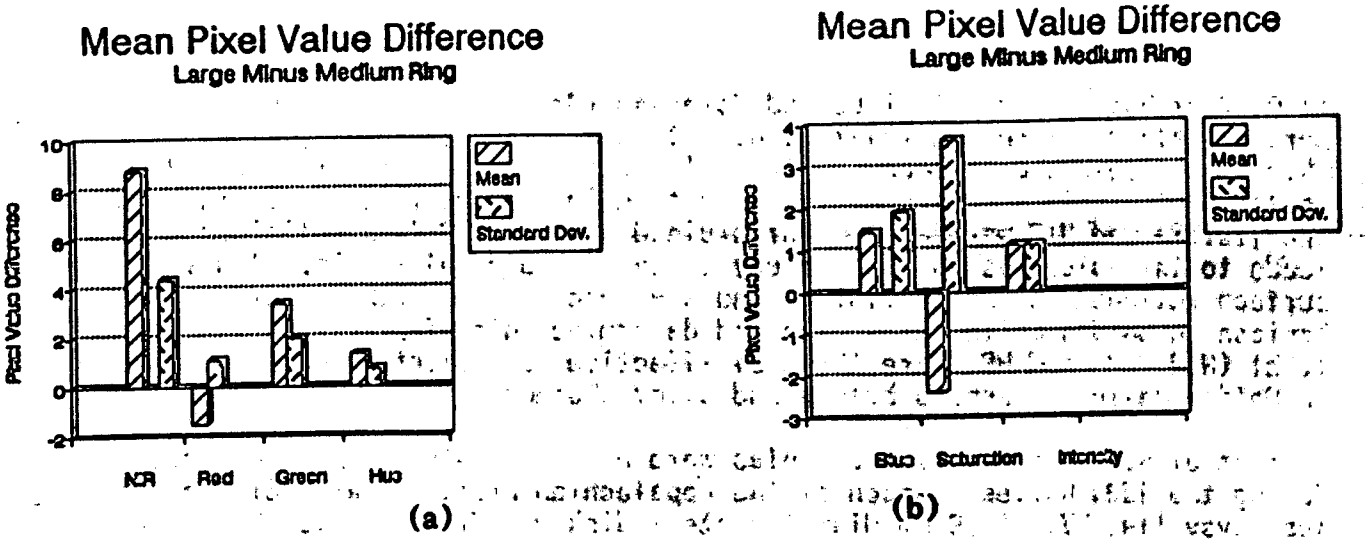

Figure 7. Mean of the differences between nonbruised profile and the bruised profile (ring 3 minus ring 2) for: a) NIR, red, green, and hue. b) Blue, saturation, and intensity.

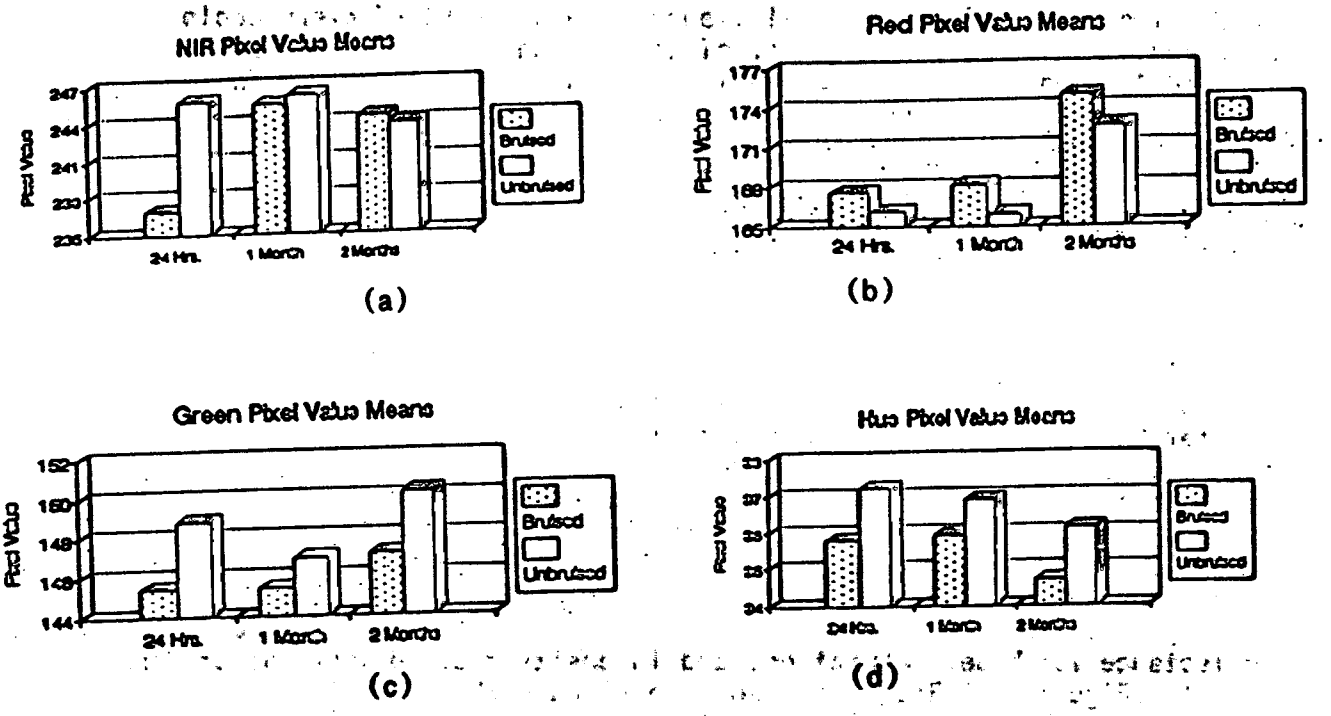

Figure 8. Mean of pixel values for ring 2 (bruised) and ring 3 (unbruised) for three storage dates after bruising for a) NIR, b) green, c) red, and d) hue.

Image processing algorithms were developed for building a database of physical properties of seeds (Cooper et al., 1985). A boundary chain code representation of a berry's profile was obtained in an attempt to detect stems in a binary image (Wolfe et al., 1985). An eight neighborhood chain code representation of a tomato's boundary was used by Sarkar et al (1985) as the feature for detecting shape. McClure et. al. (1987) started their boundary encoding algorithm with the last pixel in the center row of the scene. From this pixel an eight pixel neighborhood was searched in a clockwise direction to find the next white pixel on the boundary. The search continued until the

next white pixel was the starting pixel. Sapirstein et. al. (1987) applied an eight pixel connected region that allowed edge following of cereal kernels for inspection and classification. Sites et. al. (1988) used eight connectivity analysis to locate fruits on peach and apple trees. This analysis defined pixels to be connected if they had a common vertical, horizontal or diagonal boundary. Rehkugler et. al. (1989) used a vector oriented contour following routine to size bruises on apples. In the same paper, an algorithm that located the median pixel in each cluster row and from there searches left and right for the edge of the cluster in that row was reported. The objective of this study was to develop a method to evaluate algorithm performance for cluster boundary identification and determine which identification algorithm, CLUSTER (Rehkugler's vector oriented), CENTROID (Rehkugler's median pixel) or BOUNDARY (eight connectivity), produced the most accurate results for the least amount of processing time.

Twelve test images consisting of 256 pixel by 256 columns were generated for testing. Eleven different cluster types or shapes were identified (Figure 9).

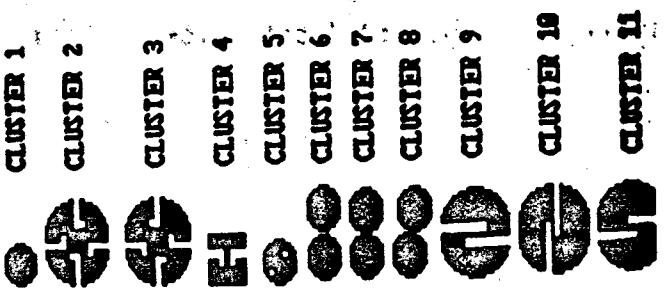

Figure 9. Eleven cluster types or shapes used to test the algorithms performance.

Each test image consisted of 10 identical clusters and each test image had a different cluster type. Clusters were black (grey level of 0) on a white background (grey level of 200). The 12th test image was a white background only. Each test cluster type was constructed with different geometric or spatial characteristics to test the ability of each algorithm to find the area and perimeter. Processing efficiency was measured in terms of processing time. Table 7 shows the area and 4-connectivity perimeter in pixels for each test cluster.

Table 7. Cluster shapes shown with the actual measured area and perimeter pixel with 4- and 8-connectivity.

Cluster Number	Measured area	4-connecitivity	8-connectivity
1	116	32	44
2	390	138	173
3	392	136	172
4	152	78	84
5	108	32	44
6	116 x 2	32 x 2	44 x 2
7	232	60	84
8	232	64	90
9	376	128	156
10	416	119	145
11	388	120	150

The cluster area, perimeter, and processing time for each test image was recorded as data. The time to scan an image with no clusters was subtracted from the images of test clusters and the resulting time was divided by 10 to find the mean time per cluster.

All of the three algorithms correctly determined the cluster area in pixels. Differences between the measured 4-connectivity perimeter and the perimeter calculated by the three algorithms is shown in Table 8.

Table 8. The results for a t-test found no significant differences between the calculated perimeters for the three tested algorithms ($p>0.2$).

Differences	N	Mean	Standard Deviation	Calculated t
CLUSTER	11	-1.286	3.068	-1.92
CENTROID	11	0.286	4.209	0.31
BOUNDARY	11	-0.857	2.056	-1.91

CENTROID was slowest algorithm, taking at least twice as long to process each cluster (Figure 10).

None of the algorithms handled clusters which had a pixel forming two different boundaries. These pixels are only counted as perimeter pixels once (test clusters 8, 9, 10, 11). CENTROID interpreted the island pixels in cluster 5 as perimeter pixels. BOUNDARY counted one of the two islands in cluster 5 as perimeter pixels because of the island's close proximity to the cluster's border. The results showed that the CLUSTER and BOUNDARY algorithms are not significantly different in performance or speed and either would be appropriate for analyzing apple bruises.

Figure 10. The time for each cluster type is shown for each algorithm.

Nonorientation System for Apple Defect Detection.

A feasibility study and preliminary design for an imaging system for non-oriented apples was undertaken (Real Time 3-D Image System, Master of Engineering Project by Wen-Chung Chen). The preliminary design employed 4 line scan cameras (a camera on each side of the apple) and appropriate lights,

a unit to detect incoming apples and scan the four cameras, and a data acquisition system.

The transport system was designed to cause the apples to pass the cameras in approximately 26ms. In order to obtain 75 scans of each of the 4 line scan cameras (64 photo-detectors), a scan rate of approximately 850KHz was needed. At this frequency, line drivers were used for data transmission over long cable lengths and under electrically noisy conditions. Lenses (25mm, F1.8 with a 0.5mm lens extension), camera (Reticon LC600 C64-2) and lights (PAR-64 bulbs) were specified. This provided a camera system with a working distance of 10 inches, a depth of field of 2 inches, and a camera with a 1.3 microwatt* sec/cm2 sensitivity. The lights needed to provide approximately 330,000 lumens for an assumed reflection rate of 30%. The data acquisition system selected was a DT2851 frame grabber board installed in an IBM-AT computer. Material, construction, and development costs were considered to high to attempt actual construction because of the reduced funding experienced by this BARD project and other research funding sources.

Time Effects and Storage Conditions on Watercore Detection.

Watercore is characterized by the filling of the large intracellular air spaces with fluid and does not generally alter the external appearance of the fruit until severe tissue breakdown occurs. Mild watercore has fluid around some of the 10 vascular bundles whereas severe watercore is characterized by the coalescing of the fluid. Currently, this damage is evaluated by visual inspection of sliced apple halves from a random sample.

Fluid filling the intracellular spaces alters the light scattering properties of apple tissue. For normal apple tissue, the presence of air spaces increases the optical path length through the fruit due to intense light scattering. Light scattering is reduced for watercore fruit and results in more energy being transmitted through the fruit (Birth and Olsen, 1964). An instrument that measured the optical-density difference at 760 and 810 nm was used to detect watercore (Birth and Olsen, 1964; Birth and Norris, 1965). This single point measurement was expanded into an area measurement by using a machine vision system (Throop et al., 1989,1991).

Severity of watercore and elapsed time before inspection affect the ability to detect watercored fruit with light transmission techniques. Researchers have reported that mild watercore has a high probability of diminishing with time, while severely watercored fruit will probably exhibit internal breakdown (Marlow and Loescher, 1984; Myers, 1983). For apples placed in regular cold storage, light transmission levels decreased to undetectable levels with initial camera settings for all classes of watercore (Upchurch et al., 1991). However, it is unknown as to the effect of storage conditions, regular cold storage versus controlled atmosphere, on the light transmission properties of watercored fruit.

Over 200 Delicious apples were segregated into four watercore classes following the procedure described by Throop et al. (1989). Class assignment was based on the amount of light that was transmitted through the fruit. Measurements were made at Cornell University prior to overnight shipment to the Georgia Experiment Station. On arrival at the Georgia Experiment

Station, light transmission levels were measured with a machine vision system. Eighty-eight apples of varying watercore were placed in controlled atmosphere (CA) storage while another 88 fruit were placed in conventional cold storage. Temperature of all fruit were maintained at 4°C.

Light transmission levels were measured at 2,4,6,10,14, and 22 weeks into the study. Apples were positioned with the stem-calyx axis collinear to a 150 W incadescent light source. While illuminating the calyx-end of the apple, a CCD camera viewed the stem-end. The mean gray level within a window that was centered about the stem was an indicator of the amount of light that was transmitted through the fruit.

Anatomical evaluation of watercored and nonwatercored tissue was performed on each sampling date. After measuring the light transmission levels, a random sample of 10 apples were removed from each storage group and destructively evaluated for visual watercore. Moisture content of watercored areas as well as nonaffected tissues was measured by vacuum oven method. Anatomical evaluation was performed on selected tissues with a scanning electron microscope (SEM). Apple tissue samples were prepared for SEM evaluation by chemical fixation and cryo-fracturing (Kim and Hung, 1990).

Preliminary results indicated that the type of storage has an affect on the amount of light transmitted through the fruit. For both CA and conventional storage, apples with no watercore had low levels of light transmitted through the fruit. Apples with severe watercore may or may not have a high light transmission score. Transmission levels appeared to remain higher for the CA group compared to the conventional storage apples. Light transmission scores for CA stored apples were not significantly different from the conventional storage scores during the first 5 sample dates (November 5 to January 2). However, a significant increase in the light transmission score was exhibited for the period January 28 to March 23. At the end of the study, light transmission scores were near zero for both treatments.

Watercored tissue exhibited anatomical differences. Initially, cells within watercored tissue were elongated when compared to cells from nonwatercored tissue. This elongation of the cells became less pronounced as storage time increased in both CA and conventional storage. Although the light transmission levels decreased to undetectable levels by April 23, watercore was still evident in some fruit; however, the fluid around the vascular bundles had changed from a translucent to a cloudy appearance. Further work is needed to ascertain the effect of watercore on cell wall structure and the effect of time on the fluid in the tissue.

DESCRIPTION OF COOPERATION

Different aspects of automatic bruise detection were addressed by the cooperators on this project. Automatic bruise detection is a very difficult research problem, and there are several areas that needed to be investigated in both basic and applied research. There were physiological changes in the apple tissue that needed to be defined. Drs. Ruth Ben-Arie, Lillian Sonego, and Nurit Flohr investigated basic physiological changes that occur when apple tissue is damaged and how these changes could be measured was a major part of their effort. The technique that has potential for automatic bruise detection

is image processing of near-infrared or color images. Limitations of near-infrared imaging as well as the problems with applying spectrophotometric results into a machine vision system were investigated by the Appalachian Fruit Research Station. In a parallel study at Cornell University, image processing algorithms were developed for distinguishing bruised from nonbruised regions in images of apples. Both near-infrared and color images were used.

Various forms of communication were used by the cooperators of this research project. Correspondence between the two countries was maintained with electronic mail (BITNET). A minimum of three meetings per year were held between Appalachian Fruit Research Station and Cornell University to review the progress of each station, and plan the following year's work.

EVALUATION OF RESEARCH ACHIEVEMENTS

The overall goal of the project was to develop a photometric measurement technique for detecting defects on apples and investigate physiological changes in damaged tissue that might lead to alternative sensing techniques. Most of the research effort concentrated on characterizing the anatomical and physiological changes that occur in techniques for detecting bruises. During the project, it became apparent that color imaging has more limitations that near-infrared imaging for detecting bruises on Golden Delicious apples. However, color imaging appears to present an advantage in detecting bruises that are over 1 month old. Time or age of the bruise is a very limiting factor for detecting bruises with near-infrared imaging. Near-infrared imaging detected bruised after 24 hours on both Red Delicious and Golden Delicious apples. For automatic bruise detection, the system must adapt and inspect for various age bruises. The physiological and anatomical studies may provide some explanations as to the changes in light reflectance experienced in these studies. To understand the changes in light reflectance over time and between varieties, there is a need for an engineer and physiologist to work very closely in relating the light interaction with the tissue condition. No effort was given toward the development of a prototype system: however, design considerations and limitations of an inspection system have been well defined by this project.

PROJECT PUBLICATIONS

Sari, Z. and J. A. Throop. 1991. Evaluation of Computational Algorithms for Measurements by Cluster Segementation. ASAE Paper 91-3053. American Society of Agricultural Engineers, St. Joseph, MI.

Throop, L. A., D. J. Aneshansley, and B. L. Upchurch. 1992. Near-IR and Color Imaging for Bruise Detection on Golden Delicious Apples. Proceedings Optics in Agriculture and Forestry, SPIE 1836-04, 12pp.

Upchurch, B. L. and J. A. Throop. 1992. Time Effects on Near-Infrared Imaging for Detecting Bruise on Apples. Proceedings Optics in Agriculture and Forestry, SPIE 1836-03, 7pp.

REFERENCES

Bilanski, W. K., C. L. Pen and D. R. Fuzzen. 1984. Apples bruise detection using optical reflectance parameters. Can. Agric. Eng. 26(2):111-114.

Brown, G. K., L. J. Segerlind, and R. Summit. 1974. "Near-infrared reflectance of bruised apples." Transactions of ASAE Vol 17(10), pp17-19.

Chen, P., McCarthy, M. J., Kauten, R. 1988. Potential use of NMR for internal quality evaluation of fruits and vegetables. ASAE Paper No. 88-6572.

Cooper, T. M. and A. G. Berlage. 1985. Machine vision for monitoring seed conditioning. ASAE paper 85-3036.

Graf, G. L. 1982. Automatic detection of surface blemishes on apples using digital image processing, pp267, Ph. D. thesis, Cornell University, Ithaca,NY, 1982.

Ingle, M. and J. F. Hyde. 1968. "The effect of bruising on discoloration and concentration of phenolic compounds in apple tissue." Proc. Amer. Soc. Hort. Sci., Vol. 93, pp738-745.

Johnson, M. 1985. Automation in citrus sorting and packing. In: Proceeding, Agrimation I., St. Joseph, MI, ASAE pp. 63068.

Klein, J. D. 1983. Physiological causes for changes in carbon dioxide and ethylene production by bruised apple fruit tissues. Ph D Diss., Michigan State Univ., East Lansing, MI.

Klein, J. D. 1987. Relationship of harvest date, storage conditions and fruit characteristics to bruise susceptibility of apple. J. Amer. Soc. Hort. Sci. 112:113-118.

Lott, R. V. 1944. "A spectral analysis of color changes in flesh and skin of maturing Grimes, Golden and Stayman Winesap apples". Proc. Amer. Soc. Hort. Sci., Vol. 44, pp157-171.

Lott, R. V. 1963. "Variability in color and associated quality constituents in Golden Delicious apple packs." Proc. Am. Soc. Hort. Sci., Vol. 83, pp139-148.

McClure, J. F. and C. T. Morrow. 1987. Computer sorting of potatoes. ASAE paper 87-6501.

Moroshima, H., Y. Seo, Y. Sagara, Y. Yamaki, and S. Matsuura. 1987. Non-destructive internal quality detection of fresh fruits and vegetables by CT scanner. In: Proceedings of the International Symposium on Agricultural Mechanization and International Cooperation in High Technology Era. Tokyo, Japan; Japanese Society of Agricultural Machinery, pp-342-349.

Pen, C. L., W. K. Bilanski, and D. R. Fuzzen. 1985. Classification analysis of good and bruise apple tissue using the measured optical reflectance. Trans. of the ASAE 18(1):326-330.

Rehkugler, G. E. and J. A. Throop. 1989. Image processing algorithms for apple defect detection. Transactions of the ASAE Vol. 32(1):267-272.

Reid, W. S. 1976. Optical detection of apple skin, bruise flesh, stem and calyx. J. Agric. Engr. Res. 21(3):291-295.

Robitaille, H. A. and J. Janick. 1973. Ethylene production and bruise injury in apple. J. Amer. Soc. Hort. Sci. 98:411-413.

Sites, P. W. and M. J. Delwiche. 1988. Computer vision to locate fruit on a tree. Transactions of the ASAE Vol. 31(1):257-263,272.

Sapirstein, H. D., M. Neuman, E. H. Wright, E. Shwedyk and W. Bushuk. 1987. An instrumental system for cereal grain classification using digital image analysis. Journal of Cereal Science 6:3-14.

Sarkar, N. and R. R. Wolfe. 1985. Feature extraction techniques for sorting tomatoes by computer vision. Transactions of the ASAE Vol. 28(3):970-974.

Taylor, R. W. and G. E. Rehkugler. 1985. Development of a system for automated detection of apple bruises. In: Proceedings, Agrimation I. St. Joseph, MI, USA, ASAE pp. 53-62.

Upchurch, B. L., H. A. Affeldt, W. R. Hruschka, K. H. Norris, and J. A. Throop. 1990. Spectrophotometric study of bruises on whole red delicious apples. Transactions of ASAE, 33(2):585-589.

Walker, J. R. L. 1964. "Studies on the enzymic browning of apples. II. Properties of apple polyphenoloxidase." Austral. J. Biol. Sci., Vol. 17, pp. 360-371.

APPENDIX A

Paper No. 91-3053
AN ASAE MEETING
PRESENTATION

EVALUATION OF COMPUTATIONAL ALGORITHMS FOR MEASUREMENTS BY CLUSTER SEGMENTATION

by

Zohar Sagi
Graduate Research Assistant
Department of Agricultural and Biological Engineering
Cornell University
Ithaca, NY 14853

James A. Throop
Research Support Specialist
Department of Agricultural and Biological Engineering
Cornell University
Ithaca, NY 14853

Written for presentation at the
1991 International Summer Meeting
sponsored by
THE AMERICAN SOCIETY OF AGRICULTURAL ENGINEERS

Albuquerque Convention Center
Albuquerque, New Mexico
June 23-26, 1991

SUMMARY:
Picture segmentation into clusters is an important image processing technique in agriculture. Three methods of determining cluster area and perimeter length are examined. The computational efficiency and accuracy of predicted area and perimeter length are used to determine the best method. Dependency of cluster characteristics such as shape, and cluster size are considered. It is found that estimation of cluster area and perimeter is very similar for the three algorithms. Time efficiency of the contour following routines (CLUSTER and BOUNDARY) is better than that of the third algorithm (CENTROID).

KEYWORDS:
image processing, segmentation, cluster, area, perimeter.

American Society of Agricultural Engineers
St. Joseph, MI 49085-9659 USA

This research was partially funded by the Binational Agricultural and Development Fund, BARD Proposal No. US-1573-88R, Photometric Imaging for Detecting Surface and Internal Defects on Apples.

Abstract

Picture segmentation into clusters is an important image processing technique in agriculture. Three methods (CLUSTER, CENTROID, and BOUNDARY) predict cluster area and perimeter length on eleven test clusters with different shapes and sizes. All of the methods accurately determine area but have equal difficulty finding perimeter length when the same pixels form two different edges. CENTROID takes twice as long to process clusters. Discussion of the 4 - connectivity and 8 - connectivity describe the problem of determining true perimeter length in digitized images.

Introduction

In recent years, image processing for agricultural applications has been widely used in research and industry. Many of these algorithms trace the boundary of clusters and determine cluster area.

Image processing algorithms were developed for building a data base of seed physical properties. After image thresholding and connectivity analysis, selected features were extracted (Cooper and Berlage, 1985). A boundary chain code representation of a berry's profile was obtained in an attempt to detect stems in a binary image (Wolfe and Sandler, 1985). An eight neighborhood chain code representation of a tomato's boundary was used by Sarkar and Wolfe (1985) as the feature for detecting shape. Guyer et. al. (1986) determined that the perimeter of a leaf is the sum of all the object pixels bordering the background and the area is the sum of all the object pixels. They do not mention the method by which they calculated the above features. McClure and Morrow (1987) started their boundary encoding algorithm with the last pixel in the center row of the scene. From this found pixel an eight neighborhood was searched in a clockwise direction to find the next white pixel on the boundary. The search continued until the next white pixel was the starting pixel. Sapirstein et. al. (1987) applied an eight connected region for edge following of cereal kernels for inspection and classification. Sites and Delwiche (1988) used eight connectivity analysis to locate fruits on peach and apple trees. This analysis defined pixels to be connected if they had a common vertical, horizontal or diagonal boundary. The actual implementation was done by a contour following technique as shown in Nevatia (1982). Pixels interior to the object's contour were considered to be part of the object. Rehkugler and Throop (1989) used a vector oriented contour following routine to size bruises on apples. In the same paper they also report about an algorithm that locates the median pixel in each row of the cluster and from there searches right and left for the edge of the cluster in that row. An eight neighbor contour following routine to detect the size of spray droplets on leaves was used by Sagi and Derksen (1991). The algorithm started with the most upper left pixel of the cluster following the contour in a clockwise direction.

Segmentation of images into clusters is a vital step in agricultural applications of image processing because of the need to determine geometric features of

objects. One of the final processing steps in those applications would be the determination of cluster perimeter and area in the digital picture. Rosenfeld and Kak (1976) mention that the definition of a perimeter of a digital picture is not trivial and give a few possibilities:

1) The sum of the lengths of the "cracks" separating points of the object (S) from it's background (S'), in other words, the number of pairs of points (p,q) with p in (S) and q in (S').

2) The number of steps taken by a border following algorithm in following the border of S.

3) The number of border points of S, i.e. the area of the border of S and S'.

Levine (1985) assumed that a border is simple, bounded and a closed curve which does not intersect with it self. All elements of the border must touch at least one pixel in the exterior set conceptually separating it from the interior. Levine concluded that a count of all pixels in the object having both '0' and '1' neighbors yields the perimeter.

Levine also stated that a discretization of an analog shape may cause errors as great as 20% in the perimeter measurements.Wechsler (1981) points out that due to the discrete grid, the perimeter measurements fluctuate according to the orientation of the object across the grid and/or the calibration factor used (scale factor between the grid size and real unit of measure). These errors could be as large as 20% when estimates of perimeter are made.

Kupla (1977) says that a contour of an object in a discrete binary image can be determined with 4 - connectivity or 8 - connectivity definitions. With the known boundary pixel located at (i,j), only pixels of a 3x3 neighborhood shown in each case in Figure 1 are checked for the next boundary pixel. The difference between the 4 - connectivity and 8 - connectivity is that for the 8 - connectivity the diagonal neighbors are considered as boundary pixels.

All of the above applications and those which have not been mentioned here use a variety of methods for determining features of clusters, none of which have shown to perform better than the others.

The objectives of this paper are:

1) Develop criteria for evaluating cluster segmentation algorithms.

2) Evaluate the performance of three cluster segmentation algorithms.

Equipment and Methods

Image analysis

Image analysis is performed on a 80286 microprocessor equipped microcomputer with a frame grabber (DT2851), a frame processor (DT2858), and a library of image processing functions (DT - IRIS) manufactured by Data Translation[1], 100 Locke Dr., Marlboro, MA 01752 is installed. The 'C'

[1] The mention of specific products is for the information of the reader only and is not considered an endorsement by Cornell University or the authors.

programming language (Microsoft C, Microsoft 16011 NE 36th Way, Redmond, WA 98073) is used for algorithm development.

Test images

Twelve test images consisting of 256 pixel rows by 256 pixel columns are generated for testing purposes. Ten identical black pixel clusters (gray level of 0) are drawn within the white background (gray level of 200) to form each image (Figure 2). Each test cluster is constructed with different geometric or spatial characteristics to test the ability of each algorithm to find the area and perimeter, during which processing efficiency is being measured in terms of processing time. Table 1 shows the area, 4-connectivity perimeter, 8-connectivity perimeter in pixels (as defined previously in the introduction), for each type of test cluster. The following is a geometric description of each test cluster (Figure 2):

1. Simple single circular cluster for timing the process for single cluster.
2. Single circular cluster with right angle protrusions pointing in a clockwise direction to check algorithm sensitivity in the clockwise direction during processing.
3. Single circular cluster with right angle protrusions pointing in a counter-clockwise direction to check algorithm sensitivity in the counter - clockwise direction during processing.
4. Single square cluster with two right angle protrusions, one pointing clockwise and the other pointing counter-clockwise, to check for problems processing right angle turns both clockwise and counter - clockwise in the perimeter.
5. Simple single circular cluster with two 4-pixel islands within, to check how the algorithm processes the island pixels.
6. Two simple circular clusters side-by-side with a single column of pixels between. This shows what effect adjacent clusters have on processing.
7. Two simple circular clusters side-by-side with no pixels between so that a single cluster is formed to test if the algorithm can recognize this geometric configuration as a single cluster.
8. Two simple circular clusters side-by-side with a single common pixel side between so that a single cluster connection is formed. This configuration tests the severest geometric shape of a single cluster perimeter.
9. Single circular cluster with two straight overlapping vertical protrusions, first from the bottom and second from the top with a single column of pixels between. This is to test both overlapping protrusions and their order of appearance in the geometric configuration of the cluster during processing.
10. Single circular cluster with two straight overlapping horizontal protrusions, first from the left and second from the right with a single row of pixels between. Same test purpose as the previous image.
11. Single circular cluster with two straight overlapping vertical protrusions, first from the top and second from the bottom with a single column of pixels between. Same test purpose as for image 9.

12. Image of the white background with no black clusters present. By processing an image without clusters, the time to scan an image without clusters can be recorded.

Testing Procedure

Testing of the three algorithms is performed by a common microprocessor. The area, perimeter, and processing time for each image is recorded as data. The time is found by placing the 'ftime' function in the algorithm immediately before and after image processing occurs so that image or data reading/writing are not included. The difference between these two times represents the image processing time. The time to scan an image without clusters is subtracted from the processing time. Since each image holds ten identical clusters, this remaining time is divided by ten to find an average computational time for each test cluster. This is necessary because the computer actually updates the clock only 18.2 times a second or approximately once every 55 milliseconds. The image processing time recorded has a tolerance of + or - 54 milliseconds. Averaging multiple readings helps to smooth out the large error from the tolerance.

Algorithm Descriptions

Contour following is intrinsically a serial operation where an error made at any step makes succeeding errors more likely. This is true of the three different algorithms named CLUSTER, CENTROID, and BOUNDARY described in this paper. Figures 3, 4, and 5 show flow diagrams for each program. BOUNDARY and CLUSTER follow the cluster edge in a clockwise direction. CENTROID locates the cluster edges from a central column of pixels within the cluster.

CLUSTER

This algorithm is the simplest of the three algorithms tested and its flow chart is shown in Figure 3. After reading the image into memory, the starting time is recorded and the image is scanned row by row, scanning the column positions left to right for each row, until a cluster edge is found or until the end of the image. If a cluster pixel is found, its position is checked for maximum and minimum row and column values and recorded. The first pixel found inside of the cluster, also called the lead pixel, and the previous pixel are examined for gray level. At this point and to completion of following the complete boundary, these rules are in effect (Figure 8).

1. If the lead pixel location is within the cluster, take one step to the left.
2. If the lead pixel location is a background pixel, take one step to the right.
3. Stop when you have found the position from which you started following the cluster edge.

Check each step for the maximum and minimum row and column position of the cluster and mark each cluster boundary pixel as a perimeter pixel by using a

different gray level from both the background and the cluster. After returning to the starting pixel, the marked perimeter pixels are checked for having a diagonal background pixel as a neighbor between two adjacent perimeter pixel neighbors (Figure 12). Remove these marked 8 - connectivity perimeter pixels and remark as cluster area pixels. Scan the image between maximum and minimum row and column positions for perimeter and cluster area pixels. Add the perimeter pixels to the area pixels to find cluster area. Store the number of perimeter and area pixels and fill in the cluster pixels with background gray level. Return to the beginning location of the cluster and continue to scan the image for more clusters. If a cluster is found, repeat the process. When the image is completely scanned for clusters, the completion time is recorded. The difference between the start and completion time is the time to process a 256 by 256 pixel image.

CENTROID

The CENTROID algorithm is different from the contour following routines in that it always locates the boundary from inside the cluster and its flow chart is shown in Figure 4. The image is read into memory and the starting time is recorded. The image is scanned row by row, checking each column position left to right for each row, until a cluster is found or until the end of the image. If a cluster pixel is found, the row is scanned until background pixels are located (Figure 9). The row value is recorded as the minimum row value and the beginning pixel position of the cluster is recorded. The beginning pixel of the row is checked as the minimum column position of the cluster and the last cluster pixel of the row is checked as the maximum column position of the cluster. At the center column position of the first row of pixels in the cluster, the row position is incremented by one. For this new row position, the column pixels to the east are checked either until there are no cluster pixels encountered or until the maximum column position has been reached, which ever is greater. This column position is checked for the maximum column location of the cluster. The row is now checked in the west direction either until there are no more cluster pixels or until the minimum column position has been reached, which ever is the least. This column position is checked for the minimum column location for the cluster. At the center of the minimum and maximum column position, increment down one row and continue the process above until a row without cluster pixels is located. The pixels within a window formed by maximum and minimum row and column positions are scanned, counted, and recorded for perimeter and area pixels. A perimeter pixel is defined as a pixel with a boundary pixel as a neighbor. Check minimum row - 1 and maximum row +1 between minimum and maximum column positions for cluster gray level pixels. If any are found, record the location and set a flag. Check minimum column - 1 and maximum column + 1 between minimum and maximum row positions for missed cluster pixels. If any are found, record the location and set a flag. The flag is now checked. If it is not set, the area and perimeter values are recorded, the cluster is filled with background pixels, and scanning of the image for new clusters continues from the

beginning location of the previous cluster. When the flag is set, the area and perimeter values are held in memory, the known part of the cluster is filled with background and processing of the cluster starts anew at the recorded location when the flag was set. This process continues increasing the area and perimeter values until a flag is no longer set. The area and perimeter are recorded and the rest of the image continues to be scanned for clusters. At the completion of image scanning, the time is recorded and the results are printed.

BOUNDARY

Boundary is the most complex of the edge following algorithms examined and its flow chart is shown in Figure 5. The image is read into memory and the starting time is recorded. The image is scanned row by row, each column position left to right for each row, until a cluster is located or until the end of the image. When a cluster pixel is found, flag 1 is set to 1 and the pixel location is checked for minimum row and column location. The discovered pixel's neighbors are now checked for boundary pixels. If the discovered pixel takes position 0 as shown in Figure 6, neighboring edge pixels are found by subtracting gray level values of the pixels located at consecutively numbered positions. Pixel value in position 1 is subtracted from pixel value in position 2. Pixel value in position 2 is subtracted from pixel value in position 3 and so on until pixel value in position 8 is subtracted from pixel value in position 9. A neighbor is considered an edge if the subtraction result is ' -1'. The new found edge pixel's neighbors are examined in this same manner until all of the boundary pixels are found. As each edge pixel is progressively found, they are marked as perimeter pixels and checked for minimum and maximum row and column positions for the cluster. There are some cases in which the current edge pixel can have two neighboring edge pixels. This case is found in test clusters 9, 10, and 11. For this case, a second flag, flag 2, is set and the location of this second edge point is stored for later processing. A series of logic statements are used to determine which edge point is processed as the primary edge pixel. The algorithm looks for new neighboring edge pixels at this new location. If no edge pixels are found but flag 2 is set, the neighbors of the pixel stored as the second edge point are checked for boundary pixels and the edge following continues from this point. If the algorithm finds no neighbors that can be edge pixels and flag 2 is not set, it is concluded that all perimeter pixels of the cluster are marked. The marked pixels within the window formed by minimum row and column, and maximum row and column positions are counted as perimeter pixels. The marked pixels are added to the rest of the pixels which form the cluster to obtain the area. The cluster pixels are filled with the background gray level and the image scan continues from the position where the first cluster pixel was found. Scanning continues to the next cluster, where the above process is repeated, or to the end of the image, whichever comes first.

Results and Discussion

A set of twelve images, as described in the introduction (Figure 2), is analyzed by the three different algorithms. Table 1 shows the true area and perimeter, in pixels, for each of the clusters examined. The true perimeter length is measured both in the 4 - connectivity and 8 - connectivity methods. Figure 7 shows an example of the difference in perimeter pixels for 4 - connectivity and 8 - connectivity measurements of the same object.

Tables 2-4 present the measurements done by each of the three algorithms. The output of each algorithm is the measured area, measured perimeter and processing time.The three algorithms determine the computed area without any errors. The area is determined from a window of minimum row and column and maximum row and column locations. Protrusions in a cluster such as those in test cluster number 11 create a problem for algorithms CENTROID and BOUNDARY. Each row, in algorithm CENTROID, is scanned right to left until background pixels are found, the column of background pixels between the protrusions of test cluster 11 stops the scanning before the correct column, thus creating a window smaller then the real window size. Algorithm BOUNDARY has a problem dealing with narrow background columns since along such columns each pixel could have a few neighboring edge pixels. BOUNDARY and CENTROID are programmed to take that into account and override such situations. Those additions to CENTROID and BOUNDARY complicate both algorithms and increased processing time per test cluster.

As for cluster perimeter, Figures 8, 9 and 10 show the typical performance of the three examined algorithms. While algorithms CLUSTER and BOUNDARY follow the boundary of the cluster in a clockwise path, algorithm CENTROID moves from row to row. Table 5 lists the differences between the measured and calculated perimeter for the test clusters. A t-test was performed (Table 6) on each of the columns in Table 5 to prove that there are no significant differences between the measured and calculated perimeter lengths for each of the three algorithms. Inspection of Table 5 shows that test clusters 5, 8, 9, 10 and 11 caused minor problems related to perimeter measurements. Algorithm CENTROID can not handle background islands within a cluster, as in test cluster 5. It determines island borders as additional perimeter pixels. BOUNDARY has difficulty with one of the island clusters because of its close proximity to the border. All three algorithms have error estimating perimeter length for clusters with narrow background columns (test clusters 8, 9, 10, 11). Those columns should have been counted twice but instead they are counted only once because of the need to mark a perimeter pixel after it is selected.

Algorithm CLUSTER marks some 8 - connected perimeter pixels (striped block in Figure 8). To determine an accurate estimation of a 4 - connectivity perimeter, the marked 8 - connected perimeter pixels are changed back to regular area pixels before the perimeter pixels are counted.

Time efficiency of CLUSTER and BOUNDARY was very similar (Figure 11). A disadvantage of algorithm BOUNDARY is that the number of calculations

per pixel, while following the contour, is almost always fixed where as the number of calculations per pixel for CLUSTER changes according to the location of the next perimeter pixel. In addition, the maximum number of calculations per pixel for CLUSTER is lower because of simplicity of the algorithm. When the test clusters are complex (test clusters 2, 3, 9, 10, 11), CLUSTER is less efficient because of the need to scan the window for marked 8 - connected perimeter pixels which have to be changed back to regular area pixels. Time efficiency of CENTROID is the poorest of the three algorithms because of duplicated operations when the rows of the clusters are scanned from right to left to find the minimum column of the window.

Conclusions

The results for a t-test found no significant differences between measured and calculated perimeters for three tested algorithms, CLUSTER, CENTROID, and BOUNDARY. The test cluster areas were all correctly measured. CENTROID is the slowest algorithm, taking at least twice as long to process each cluster. None of the algorithms can handle clusters which have the same perimeter pixels forming two different boundaries. The marked perimeter pixels are not counted twice (test clusters 8, 9, 10, 11). CENTROID interpreted the island pixels in test cluster 5 as perimeter pixels. BOUNDARY counted one of the two islands in test cluster 5 as perimeter pixels because of the island's close proximity to the cluster's border. The results prove that algorithms CLUSTER or BOUNDARY are recommended for use in general applications where geometric features are needed. If one is interested in an 8 - connected region as the estimator for perimeter length, simple logic has to be added to the algorithms. The basic idea would be to scan the window and look for any pixel which has 4 - connected perimeter neighbors on two adjacent sides and has a diagonal background neighbor (Figure 12). It should also be understood that if estimation of the smooth (continuous) original perimeter is desired, one has to use a compensation factor based on the 4 or 8 - connectivity definitions (Kupla, 1977).

References

Cooper, T. M. and A. G. Berlage. 1985. Machine Vision for Monitoring Seed Conditioning. ASAE paper 85-3036.

Guyer, D. E., G. E. Miles, M. M. Schreiber, O. R. Mitchell and V. C. Vanderbilt. 1986. Machine Vision and Image Processing for Plant Identification. Transaction of the ASAE Vol. 29(6):1500-1507.

Kupla, Z. 1977. Area and Perimeter Measurements of Blobs in Discrete Binary pictures. Computer Graphics and Image Processing 6: 434-454.

Levine, M. D. 1985. Vision in Man and Machine. McGrew-Hill, Inc.

McClure, J. F. and C. T. Morrow. 1987. Computer Sorting of Potatoes. ASAE paper 87-6501.

Nevatia, R. 1982. Machine Perception. Prentice-Hall, Inc.

Rehkugler, G. E. and J. A. Throop. 1989. Image Processing Algorithms for Apple Defect Detection. Transaction of the ASAE Vol. 32(1):267-272.

Rosenfeld, A. and A. C. Kak. 1976. Digital Image Processing. Academic Press.

Sites, P. W and M. J. Delwiche. 1988. Computer Vision to locate Fruit on a Tree. Transactions of the ASAE Vol. 31(1):257-263, 272.

Sagi, Z. and R. C. Derksen. 1991. Machine Vision and Image Processing for Spray Distribution Analysis. ASAE paper 91-3050.

Sapirstein, H. D., M. Neuman, E. H. Wright, E. Shwedyk and W. Bushuk. 1987. An Instrumental System for Cereal Grain Classification using Digital Image Analysis. Journal of Cereal Science 6:3-14.

Sarkar, N. and R. R. Wolfe. 1985. Feature Extraction Techniques for Sorting Tomatoes by Computer Vision. Transactions of the ASAE Vol. 28(3):970-974 and 979.

Wechsler, H. 1981. A New and Fast Algorithm for Estimating The Perimeter of Objects for Industrial Vision Tasks. Computer Graphics and Image Processing 17: 375-385.

Wolfe R. R. and W. E. Sandler. 1985. An Algorithm for Stem Detection Using Image Analysis. Transactions of the ASAE Vol. 28(2):641-644.

Cluster Number	Measured area	4 - connecitivty	8 - connectivity
1	116	32	44
2	390	138	173
3	392	136	172
4	152	78	84
5	108	32	44
6	116 x 2	32 x 2	44 x 2
7	232	60	84
8	232	64	90
9	376	128	156
10	416	119	145
11	388	120	150

Table 1: Actual measured area and perimeter of test clusters.

Cluster	Area (pixels)	Perimeter (pixels)	Process Time (sec)	Cluster Process Time
1	116	32	1.16	0.028
2	390	138	1.81	0.093
3	392	136	1.87	0.094
4	152	78	1.32	0.044
5	108	32	1.16	0.028
6	116 x 2	32 x 2	1.43	0.055
7	232	60	1.43	0.055
8	232	62	1.43	0.055
9	376	117	1.81	0.093
10	416	112	1.81	0.093
11	388	113	1.87	0.099
12	0	0	0.88	

Table 2: Performance of CLUSTER.

Cluster	Area (pixels)	Perimeter (pixels)	Process Time (sec)	Cluster Process Time
1	116	32	1.42	0.071
2	390	138	3.35	0.264
3	392	136	3.29	0.258
4	152	78	1.82	0.111
5	108	45	1.49	0.078
6	116 x 2	32 x 2	2.20	0.149
7	232	60	1.92	0.121
8	232	62	2.09	0.138
9	376	120	3.19	0.248
10	416	115	3.30	0.259
11	388	124	7.14	0.643
12	0	0	0.71	—

Table 3: Performance of CENTROID.

Cluster	Area (pixels)	Perimeter (pixels)	Process Time (sec)	Cluster Process Time
1	116	32	1.26	0.043
2	390	138	1.70	0.087
3	392	136	1.65	0.082
4	152	78	1.31	0.048
5	108	37	1.21	0.038
6	116 x 2	32 x 2	1.53	0.070
7	232	60	1.48	0.065
8	232	62	1.48	0.065
9	376	120	1.70	0.087
10	416	115	1.65	0.082
11	388	116	1.71	0.088
12	0	0	0.83	—

Table 4: Performance of BOUNDARY.

Cluster Number	CLUSTER	CENTROID	BOUNDARY
1	0	0	0
2	0	0	0
3	0	0	0
4	0	0	0
5	0	13	5
6	0	0	0
7	0	0	0
8	-2	-2	-2
9	-11	-8	-8
10	-7	-4	-4
11	-7	4	-4

Table 5: Differences between measured 4 - connectivity perimeter and calculated perimeter for the three algorithms.

Differences	N	Mean	Standard Deviation	Calculated t
CLUSTER	11	-1.286	-3.068	-1.92
CENTROID	11	0.286	4.209	0.31
BOUNDARY	11	-0.857	2.056	-1.91

Table 6: Statistical analysis of differences between measured and computed perimeter. The t-value for 10 degrees of freedom at a confidence level of 99% is 3.169 .

	i-1,j	
i,j-1	i,j	i,j+1
	i+1,j	

a

i-1,j-1	i-1,j	i-1,j+1
i,j-1	i,j	i,j+1
i+1,j-1	i+1,j	i+1,j+1

b

Figure 1: a) 4 - connectivity neighborhood, b) 8 - connectivity neighborhood.

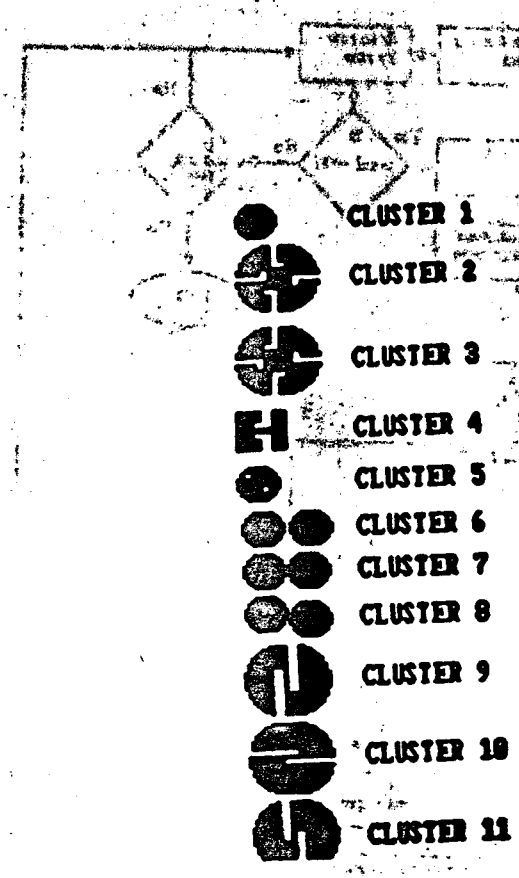

Figure 2: Test clusters.

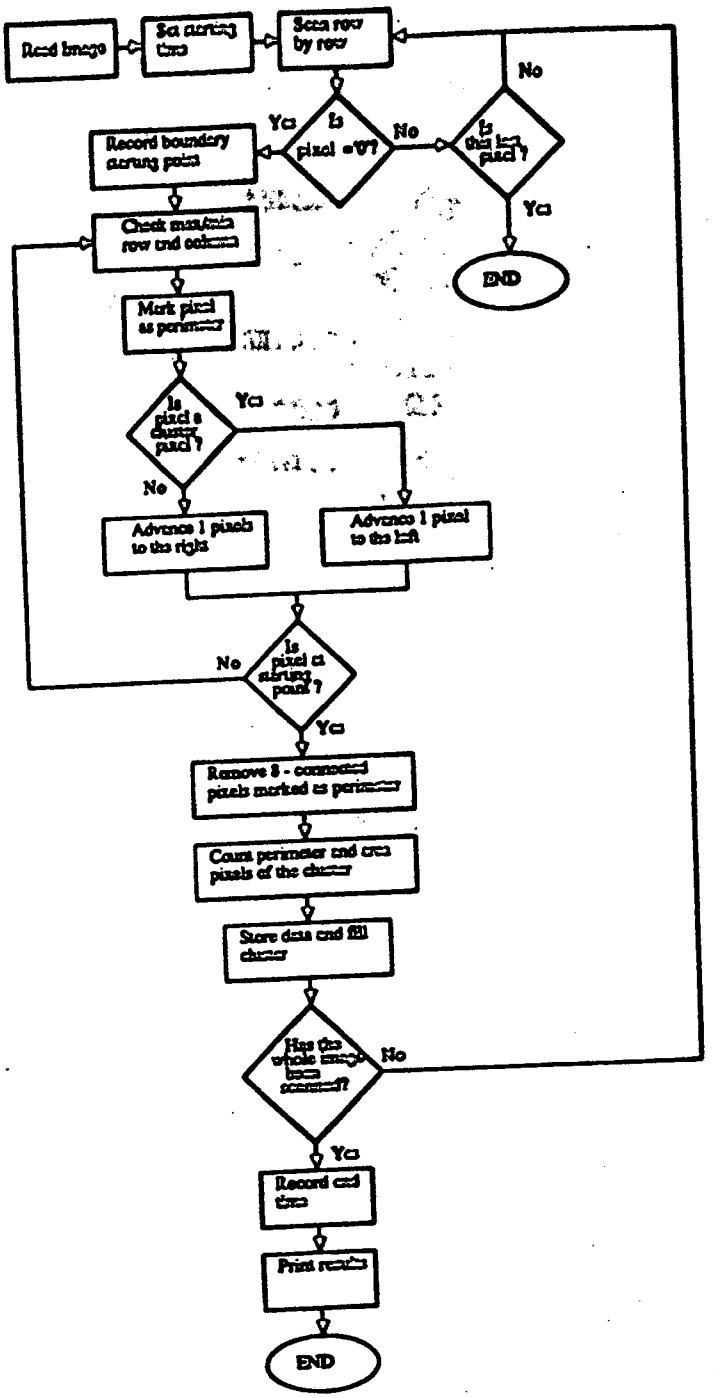

Figure 3: Flow chart of algorithm CLUSTER.

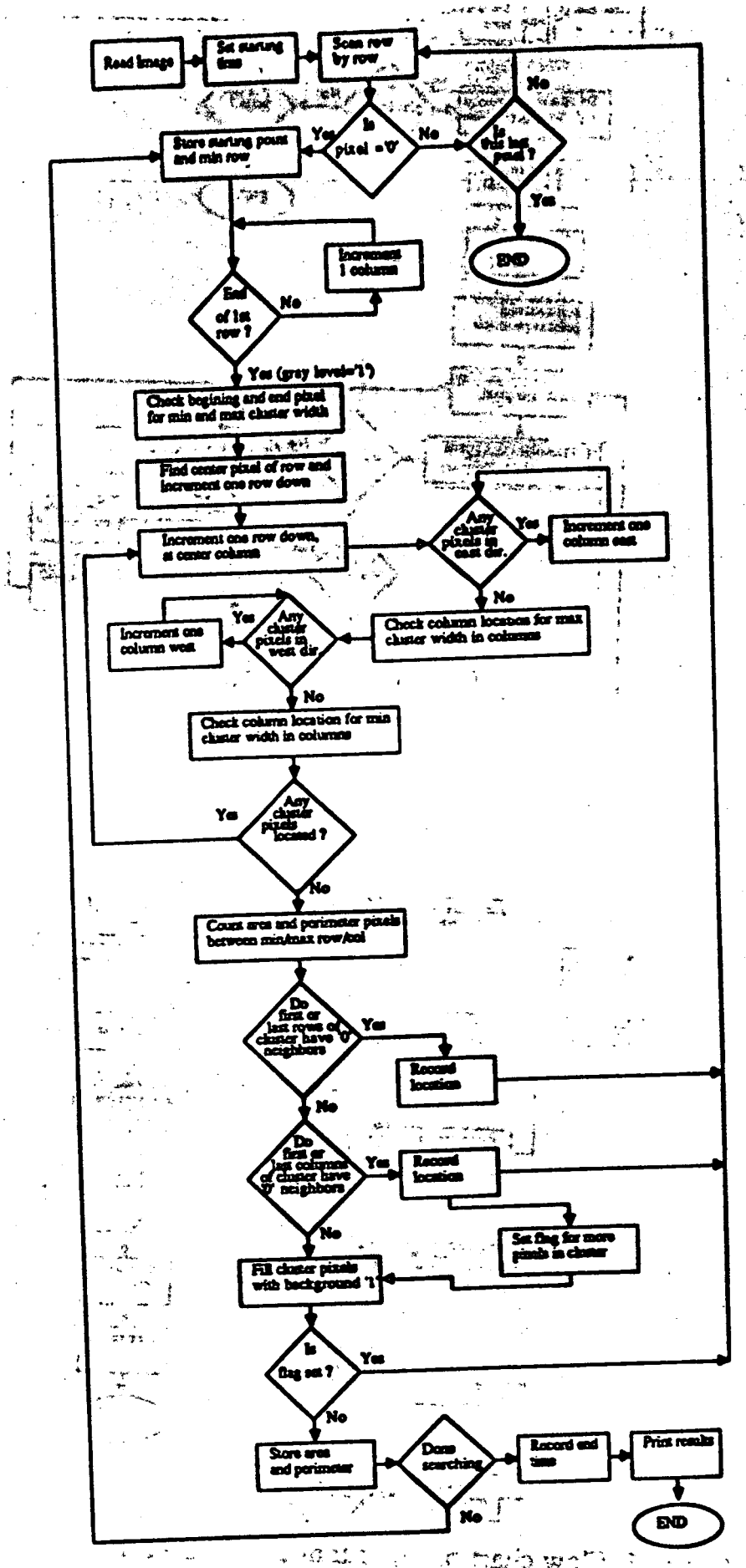

Figure 4: Flow chart of algorithm CENTROID.

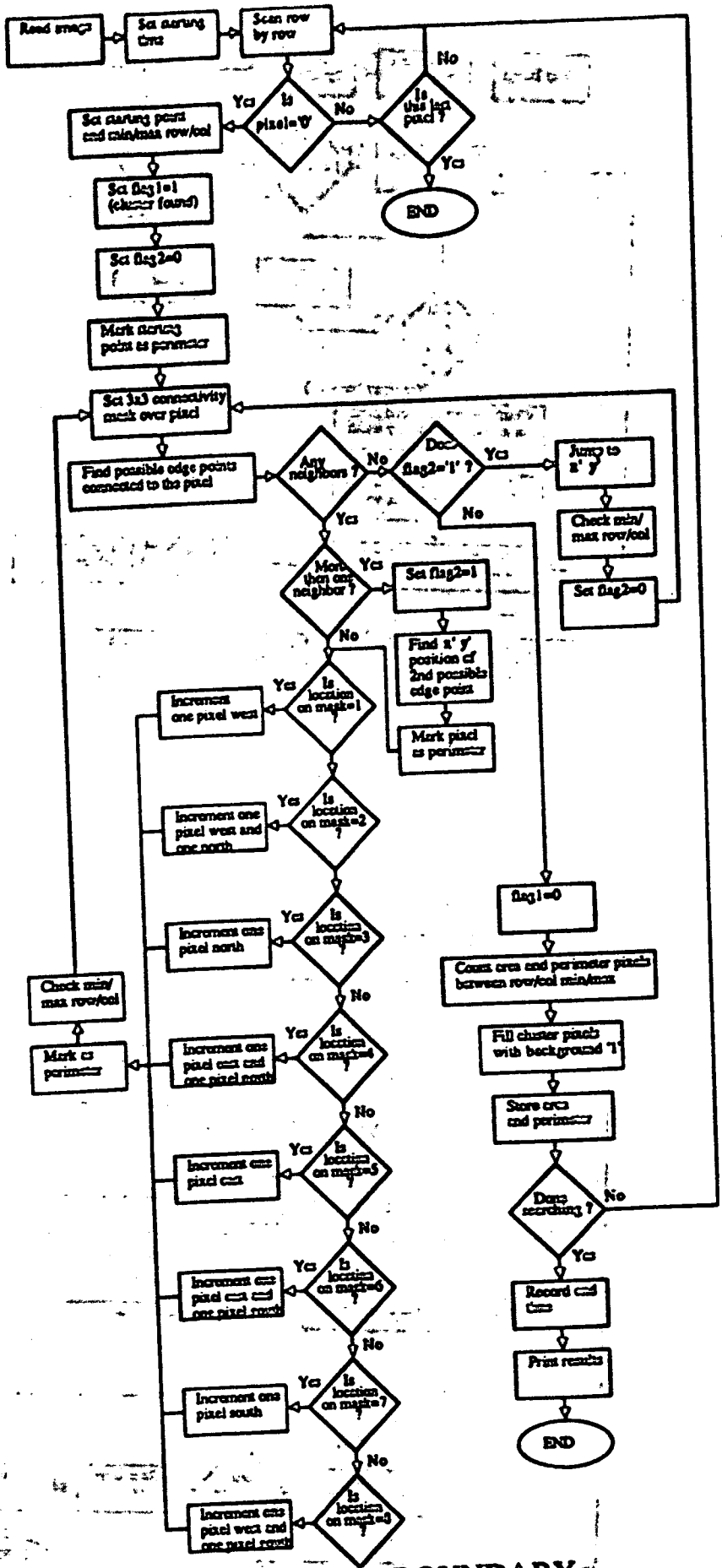

Figure 5: Flow chart of algorithm BOUNDARY.

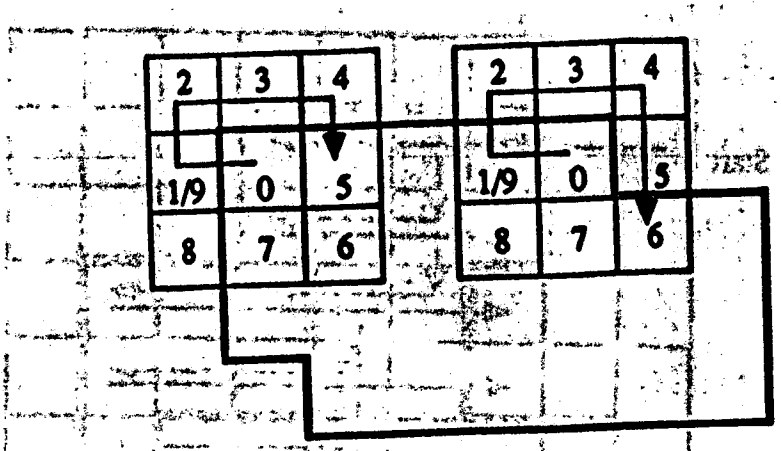

Figure 6: Selecting the next edge pixel with BOUNDARY.

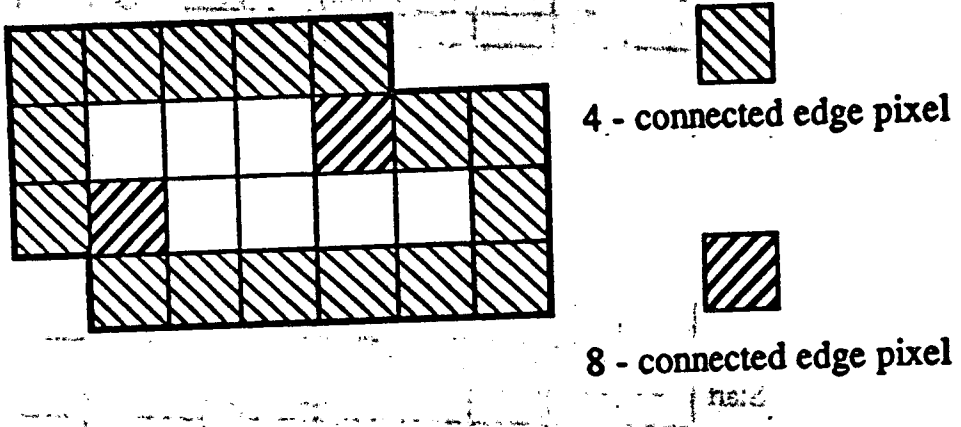

Figure 7: Perimeter pixels.

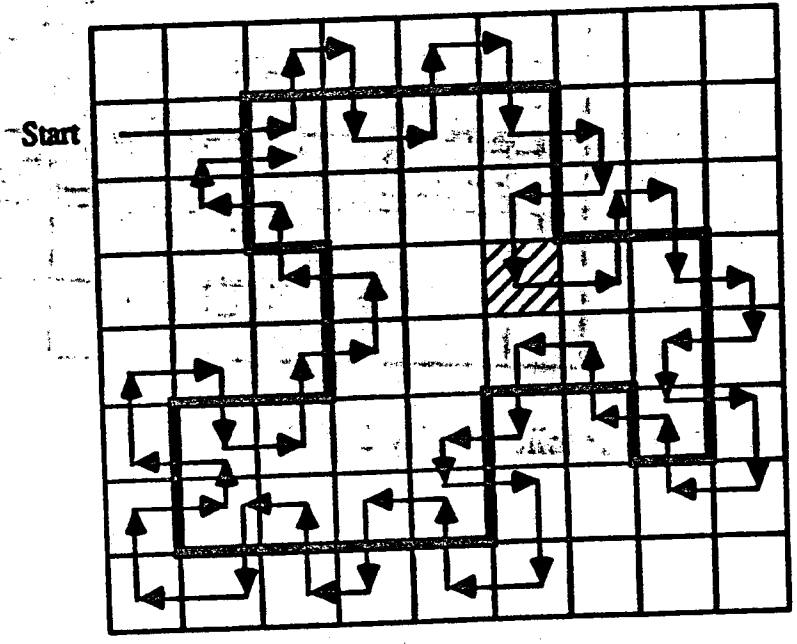

Figure 8: Contour following by CLUSTER.

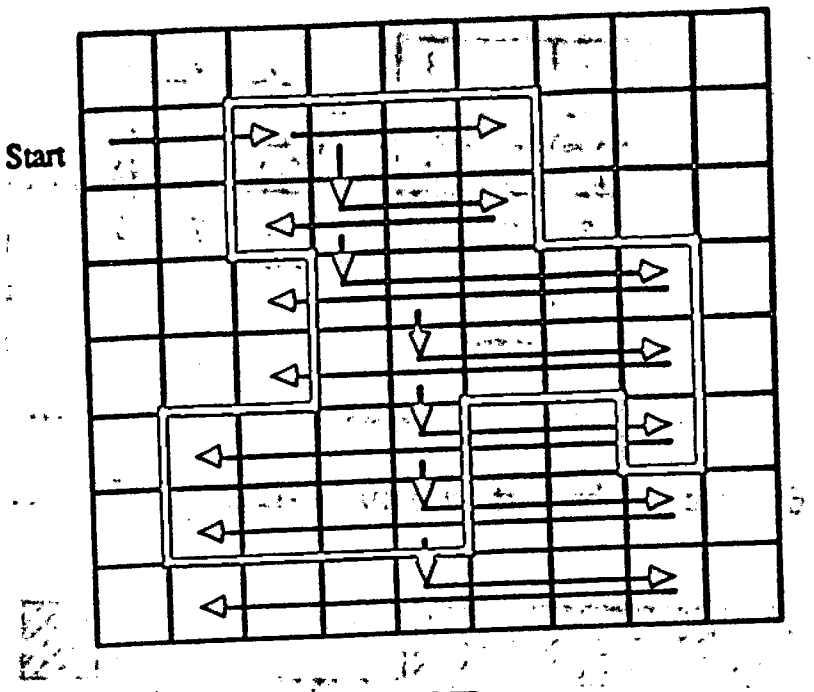

Figure 9: Window selection for CENTROID.

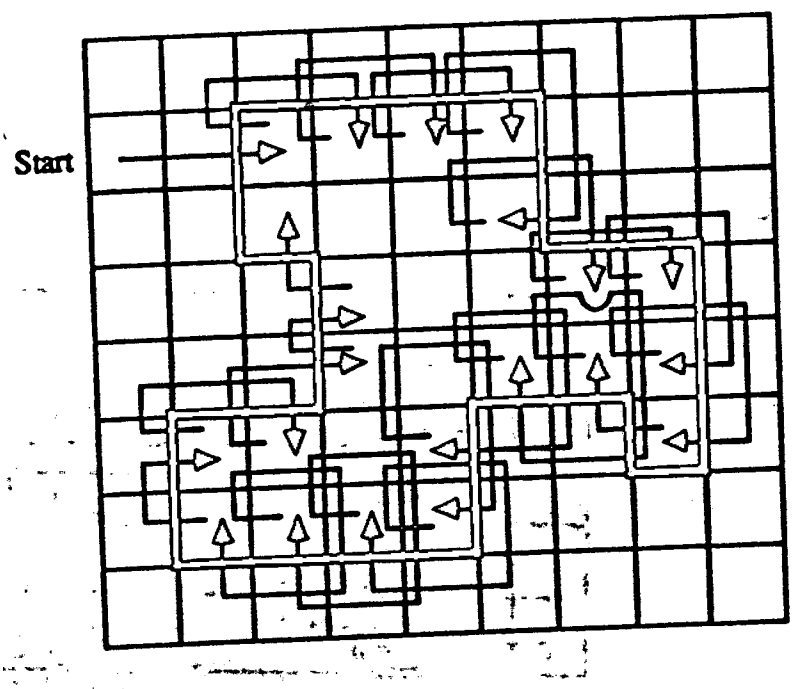

Figure10: Contour following by BOUNDARY.

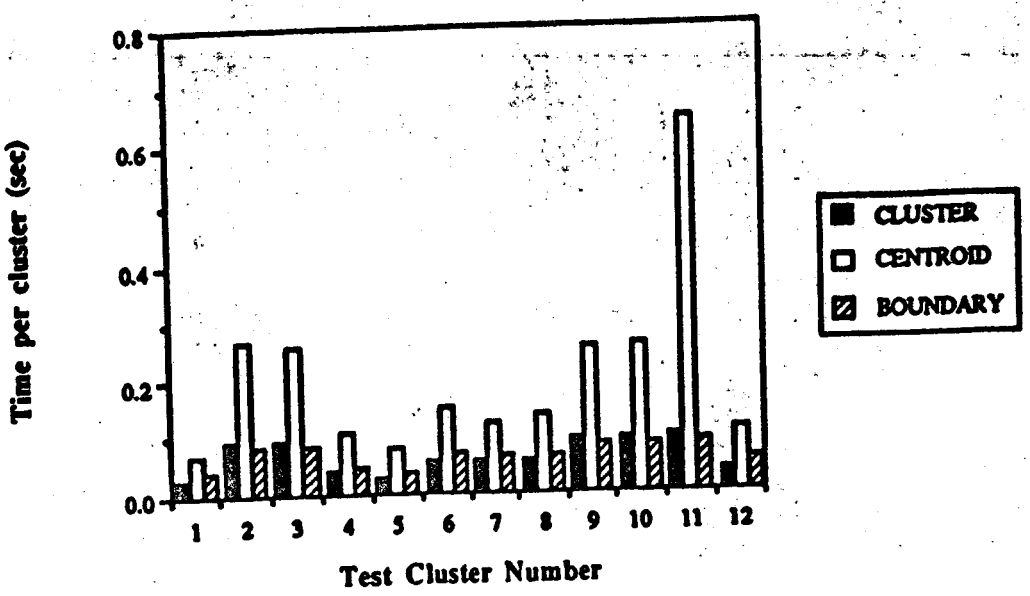

Figure 11: Processing time per cluster.

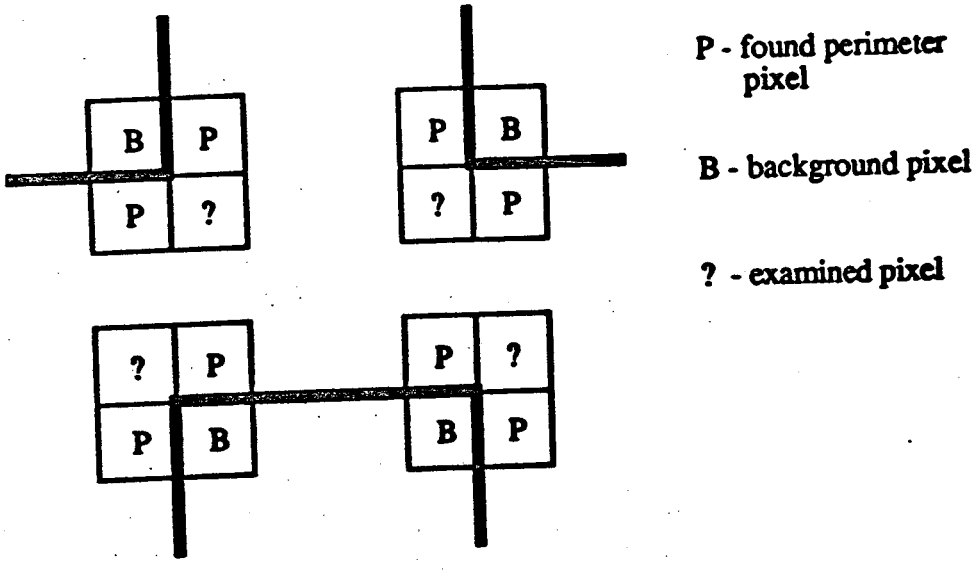

Figure 12: Location of 8 - connected perimeter pixels.

APPENDIX B

Near - IR and color imaging for bruise detection on Golden Delicious apples

James A. Throop, Daniel J. Aneshansley
Cornell Unversity, Department of Agricultural and Biological Engineering, Ithaca, New York 14853

Bruce L. Upchurch
USDA-ARS Appalachian Fruit Research Station
Kearneysville, West Virginia 25430

ABSTRACT

Digital images of reflected light in both the near - infrared (NIR) and visible wavelengths from the surface of bruised and unbruised Golden Delicious were captured for classifying bruise damage. Each of the attributes of two models for color representation, RGB and HSI, were compared to NIR for their ability to discriminate bruised from unbruised tissue. The surface reflectance for good tissue decreased from the fruit center outward, except saturation which increased. Reflectance of good tissue also varied adjacent to the bruised area compared to a location 60 degrees away. NIR, green, hue and red were the features which showed the most contrast between bruised and undamaged tissue. This contrast did not decrease for green, red, and hue as storage time increased.

INTRODUCTION

The appearance of a Golden Delicious apple is the primary factor on which the consumer makes a purchasing decision. The consumer expects bruise and blemish free fruit. The eye is a sensitive sensor of spectral reflectance from the apple surface to judge overall quality. As the technology became available, it was only natural for scientists to measure surface reflectance to quantify apple quality and maturity. Early work used the spectral reflectance for wavelengths from 400 - 700nm to characterize changes in color as the fruit matures.[1,2,3] This information was used to measure ripeness on Golden Delicious.[4] The values were converted to CIE chromaticity values and correlated with picking dates.

Mechanical injury of Golden Delicious apples can result in softening and discoloration of the tissue under the apple's skin. The discoloration or browning of fruits is ascribed to the oxidation and polymerization of phenolic compounds.[5,6] Unlike red cultivars which tend to mask the browning, the partially translucent yellow skin of Golden Delicious apples allows the browning to show through the skin in sharp contrast to the uniform fruit color. Spectral reflectance at 600nm was used to measure browning on Golden Delicious apples and was correlated with time and temperature.[7] Discoloration was expressed as the difference between normal and injured tissue reflectance.[7] Golden Delicious were found to discolor erratically and more slowly than other

cultivars and temperature was found to have little effect on the rate of browning.[7] The reduction in surface reflectance between normal and bruised tissue for Golden Delicious was found to be about 8% compared to 11% for red cultivars such as Red Delicious and McIntosh.[8] Surface reflectance using wavelengths between 700 - 2200nm was reduced for bruised compared to normal Golden Delicious tissue.[8] The signifigance of this finding is that it removed color variations from the reflectance measurement for bruised tissue. The reflectance properties for peeled and unpeeled Golden Delicious were found for the wavelength range 350 to 800 nm.[9] All of the above surface reflectance measurements were made with spectrophotometers and would not be applicable to high speed measurement required in packing lines.

Digital image processing was developed to measure surface reflectance over the total fruit surface to find areas of lower surface reflectance which could be bruises.[10] This method could rapidly measure surface reflectance of a stream of apples on the packing line. Linear discriminate classifiers were determined by using a training set of apples with known bruise areas.[10] Predicting bruised tissue on Golden Delicious apples by measuring the NIR surface reflectance for wavelengths between 750nm to 850nm showed correlations to actual bruising of 0.22 compared to 0.72 or better for Red Delicious and McIntosh.[10] When the apples were cut after testing, a layer of good tissue cells was found just under the skin of the Golden Delicious; unlike Red Delicious and McIntosh which had damaged cells.[10] This observed reduction in surface reflectance in both the visible and NIR wavelengths for bruised tissue on Golden Delicious apples leads to the objective of this research. An automatic detection system to size and find defects on Golden Delicious apples using data reduction enabled apples to be scanned at a rate of five fruit per second but could not separate bruised fruit.[11]

OBJECTIVE

Examine digital imaging of diffuse surface reflectance both in the visible and NIR spectrums as methods for detecting bruises on Golden Delicious apples. Determine which features of reflected light (NIR,RGB,and HSI) are the most effective for detecting damaged tissue on Golden Delicious apples before and after storage.

MATERIAL AND METHODS

Two samples of 88 Golden Delicious apples were hand harvested in mid-September during the 1991 harvest season at the Applachian Fruit Research Station in Kearneysville, WV. Each apple was placed in tray packs and stored in a cold room at 1^0 C until needed for testing. A 39 mm diameter steel disk was dropped[12] onto the surface of each fruit. Samples were held for 24 hours at 20^0 C to allow full bruise development and then digital images were captured (time 1). Thereafter, images were grabbed twice at one month intervals (time 2 and time 3). The apples were removed from cold storage 24 hours prior to imaging and held at 20^0 C.

A slightly translucent arcylic plastic diffuser mounted in front of

eight tubular tungsten lamps ([1]General Electric 40A, 40 W) mounted in the apple lighting chamber provided uniform diffuse illumination of the apple surface.

Color images of one sample of 88 apples were acquired by digitizing the output from a RS-170 solid-state camera. A DEC-IPS (Kontron Electronics) image processing system connected to a MicroVax II (Digital Equipment Corp) was used to acquire RGB color images. The DEC-IPS consisted of a frame grabber, image processor, video memory, and image processing software. A 25mm lens with an aperture set at f4.0 was mounted to a color CCD camera (Model M-852, Micro Technica). To standardize images from one date to another, the gain for each color band was adjusted while viewing a Teflon cylinder. Each color band was independently adjusted to a mean grey level: red-142, green-199, blue-189. The RGB images were transported to a PC-based system equipped with a frame grabber (DT2871), frame processor (DT2858), and a library of image processing functions (AURORA, Data Translation Inc.) where they where converted to HSI color images.

NIR images were acquired of a second sample of 88 apples by digitizing the RS-170 output of a CCD array camera (Model 4810, COHU Electronics). A PC-based system equipped with a frame grabber (DT2851), frame processor (DT2858), and image processing library functions (DTIRIS, Data Translation Inc) captured the NIR images. A 25mm lens with an aperture set at f1.4 was mounted to the camera with a long pass filter (Kodak Wratten 89B) placed in front of the lens to limit the light viewed by the camera to the NIR wavelengths.[4]

Two 512 vertical pixel x 512 horizontal pixel images of every apple were acquired; one with the bruise centered on the axis of the lens and a second with the bruise rotated (about the apple's stem/calyx axis) 60 degrees away from the lens axis displaying only undamaged tissue.

Image processing of all of the images consisted of interactively locating and recording the location of the center of the bruised area. The mean pixel value (0 to 255) of pixels at 1 degree intervals about the circumference of three concentric rings of three different diameters were recorded. Figure 1 shows the location and relative size of the three rings. Ring 1 had a fixed diameter of 10 pixels. Ring 2 had an approximate diameter equal to the bruise diameter (80-90 pixels or 20-25mm) minus 25 pixels. Ring 3 had an approximate diameter equal to the bruise diameter plus 25 pixels. The mean pixel values for both bruised and unbruised tissue (apple rotated 60^0) centered on the location of the bruise center were recorded for NIR, RGB, and HSI Golden Delicious apple images captured at the three different storage times.

---

[1] Mention of specific products is for the information of the reader only and is not considered an endorsement by Cornell University, USDA-ARS, or the authors.

RESULTS AND DISCUSSION

To determine the variations in reflectance from the surface at the apple's center outward to the apple's edges, a two sample t-test was performed to determine if the mean pixel values of the three concentric rings located on unbruised tissue are different from each other. Figures 2 and 3 show the mean pixel values of unbruised tissue for the three rings located at 60 degrees to the bruise center. It was found that the means for ring 3 were significantly different from means of rings 1 and 2 ($p<0.01$), specifically higher for NIR, green, blue, hue, saturation and intensity and lower for red. The same test was performed on rings 1 and 2 (0 degrees), bruised tissue, which determined that the means for NIR and hue were significantly different for the two ring sizes ($p<0.05$). For all tests except saturation, as the ring diameter increased, there was a trend of the mean pixel value declining. Saturation showed the reverse, as the ring diameter increased, the mean pixel value showed an increasing trend. Therefore, there is a geometric effect because of the surface curvature of the apple.

The reflectance variability of undamaged tissue values around each fruit may vary from location to location. The mean pixel values of the two largest rings (ring 3 at 0 and 60 degrees) were compared. Comparing the mean values for these rings in Figures 2 and 3 shows that the mean pixel value for red, green, blue, hue, saturation, and intensity for unbruised tissue was significantly different ($p<0.01$). This test showed that there was less red, more green, more blue, greater hue, less saturation, and more intensity on the unbruised side of the sample compared to the bruise side. The sample could have been by chance a different color on one side compared to the other or there could be effects on the reflectance from the large ring of undamaged tissue around the bruised area caused by internal interactions in undamaged cells adjacent to bruised tissue.

Because of the reflectance difference from the smallest (ring 1) to the largest ring (ring 3) and the variations found for the two large rings spaced 60 degrees apart, it was decided that the best contrast for comparing bruised and undamaged tissue would be found between ring 2 inside the bruise and ring 3 located just outside and concentric with the bruise. Figure 4 shows the mean found by averaging the difference of the mean pixel values of the two rings for each apple. The standard deviations are also shown. A t-test was performed to see which mean had the greatest difference from 0. NIR was found to have the greatest difference, followed in descending order by hue, green and red. Saturation, blue and intensity were found to be different from 0, but by a much smaller t-value caused mainly by their large standard deviations. NIR, green, hue and red show the most promise as reflectance features which could be used to discriminate between bruised and undamaged tissue.

Figures 5 and 6 show the changes for the reflectance features for bruised and undamaged tissue for ring 2 and ring 3 over a two month period. NIR reflectance for bruised tissue increased in the first month of storage to a value nearly equal to undamaged tissue. NIR reflectance

for undamaged tissue varied only slightly over the same period. The mean pixel value for bruised and unbruised tissue increased equally for red and decreased equally for hue. The differences in pixel values between damaged and undamaged tissue for these two features remained constant over the storage period. Blue, saturation, and intensity showed a reduced contrast between pixel values for bruised and unbruised tissue. Green showed a decrease in mean pixel values for time 2 for unbruised tissue and an equal value for bruised tissue. This resulted in a lower difference in contrast between the tissue types for time 2 only. Time 3 showed the same contrast between bruised and undamaged tissue as time 1. The color features of red, green, and hue are not effected as much by storage time as NIR. These features maintained a difference between bruised and unbruised tissue over the total storage time and may be possible features to form a discriminate function for identifying bruising on stored Golden Delicious.

CONCLUSIONS

Surface reflectance for Golden Delicious was found to decrease significantly from the fruit center outwards for the reflectance features of NIR, red, green, blue, hue, and intensity. Saturation was found to increase.

A color difference for good tissue was found between two locations, one concentric about the bruise and the other 60 degrees apart. From the data collected it was not possible to tell if this difference was an interaction from the bruising process in good tissue adjacent to bruised tissue or was a natural color variation.

NIR, hue, green, and red were more effective for discriminating bruised from undamaged tissue. Large variations in surface reflectance for blue, saturation, and intensity reduced their discriminating ability.

Red, green and hue, unlike NIR, did not show the increase in reflectance with storage time. These features could be used to form a discriminate function for identifying bruising on stored Golden Delicious apples.

ACKNOWLEDGEMENTS

This research was supported by Grant No. US-1573-88R from BARD, The United States-Isreal Binational Agricultural Research & Development Fund.

REFERENCES

1. R. V. Lott, "A spectral analysis of color changes in flesh and skin of maturing Grimes, Golden and Stayman Winesap apples". Proc. Amer. Soc. Hort. Sci., Vol. 44, pp. 157-171, 1944.

2. R. V. Lott, "Variability in color and associated quality constituents in Golden Delicious apple packs." Proc. Am. Soc. Hort. Sci., Vol. 83, pp. 139-148, 1963.

3. R. V. Lott, "Changes in skin color during the ripening of Golden Delicious apples, in relation to harvesting at different stages of maturity." Hort. Res. Vol. 6, pp. 113-125, 1966.

4. D. R. Bittner and K. H. Norris, "Optical properties of selected fruits vs maturity." Quality Detection in Foods, pp. 57-64, American Society of Agricultural Engineers, St. Joseph, MI. 1976.

5. J. R. L. Walker, "Studies on the enzymic browning of apple fruits." New Zeal. J. Sci., Vol 5, pp. 316-324.

6. J. R. L. Walker, "Studies on the enzymic browning of apples. II. Properties of apple polyphenoloxidase." Austral. J. Biol. Sci., Vol. 17, pp. 360-371, 1964.

7. M. Ingle and J. F. Hyde, " The effect of bruising on discoloration and concentration of phenolic compounds in apple tissue." Proc. Amer. Soc. Hort. Sci., Vol. 93, pp. 738-745, 1968.

8. G. K. Brown, L. J. Segerlind, and R. Summit, "Near-infrared reflectance of bruised apples." Transactions of ASAE Vol 17(10), pp. 17-19, 1974.

9. W. S. Reid, "Optical detection of apple skin, bruise, flesh, stem, and calyx." J. Agric. Engng. Res., Vol. 21, pp. 291-295, 1976.

10. G. L. Graf, Automatic Detection of Surface Blemishes on Apples Using Digital Image Processing, pp. 267, Ph. D. thesis, Cornell University, Ithaca, NY, 1982.

11. A. Davenel, Ch. Guizard, T. Labarre, and F. Sevila, "Automatic detection of surface defects on fruit by using a vision system." J. Agric. Engng. Res., Vol. 41, pp. 1-9, 1988.

12. B. L. Upchurch, H. A. Affeldt, W. R. Hruschka, K. H. Norris and J. A. Throop, "Spectrophotometric study of bruises on whole Red Delicious apples." Transactions of the ASAE, Vol. 33,(2), pp. 585-589, 1990.

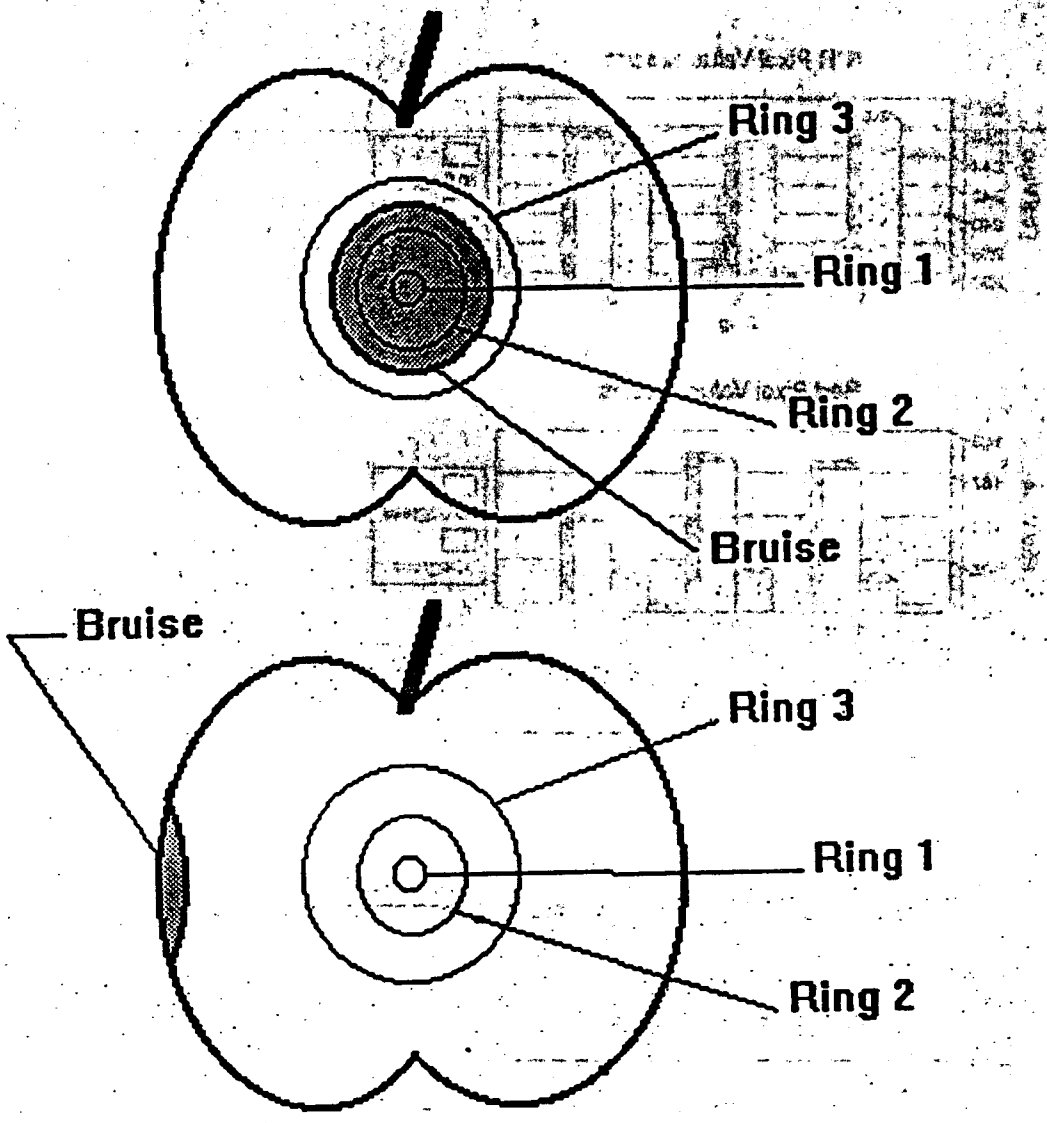

Figure 1. Diagram showing the location of the rings of pixels averaged to determine a mean pixel value for reflectance for bruised and unbruised tissue on Golden Delicious apples.

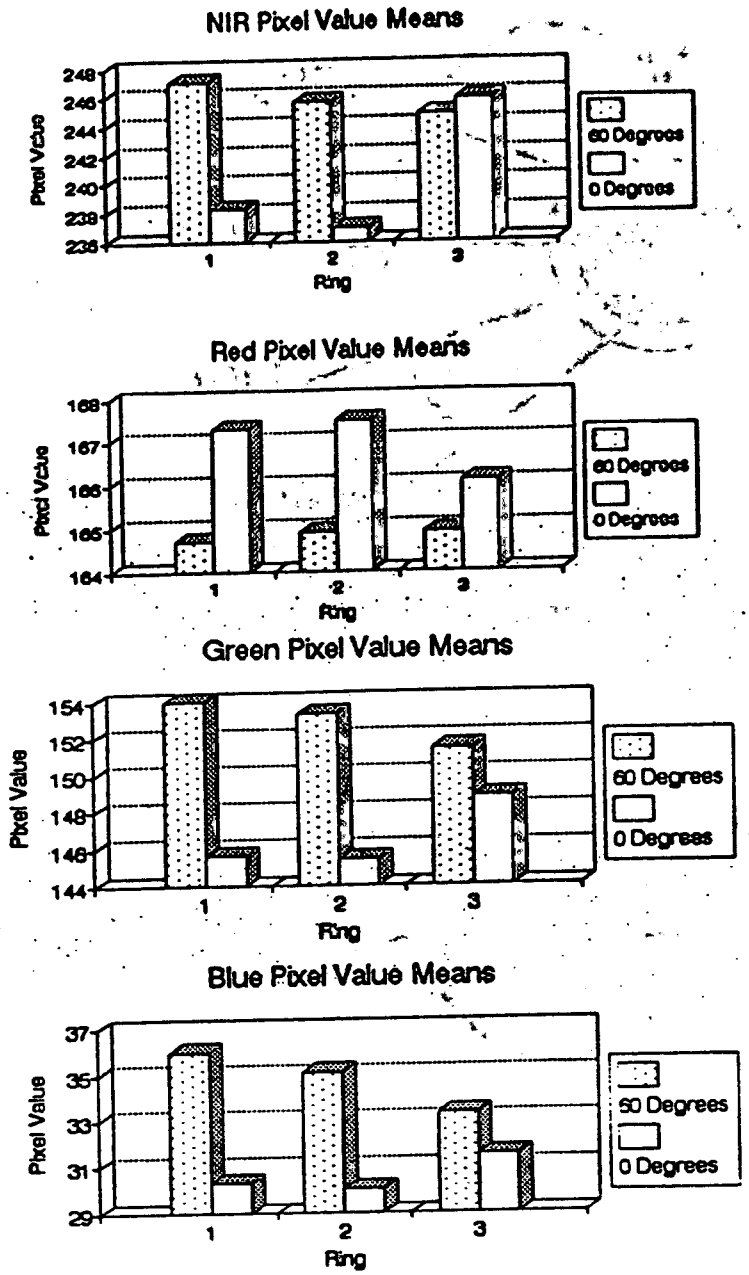

Figure 2. Surface reflectance (pixel values) 24 hours after bruising for NIR, red, green, and blue for three concentric rings both centered and 60 degrees from the bruise center are shown. Ring 1 is the smallest and ring 3 the largest. Ring 3 at 0 degrees and rings 1-3 at 60 degrees represent values for undamaged tissue.

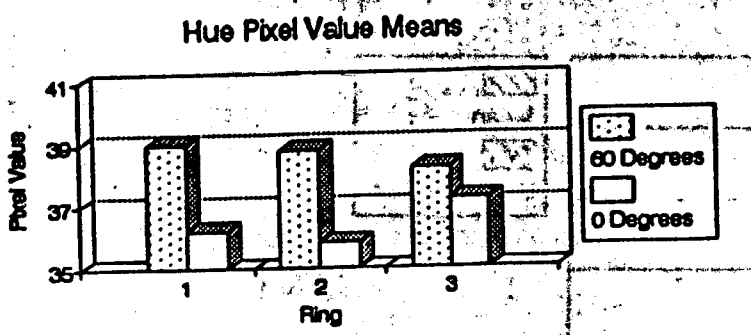

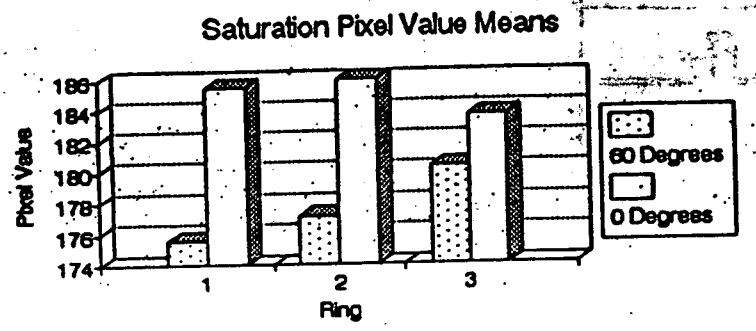

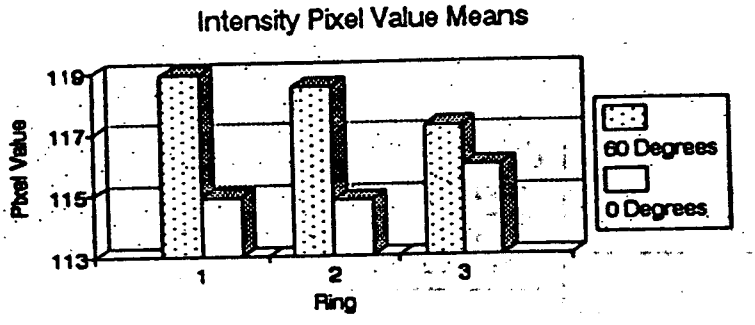

Figure 3. Surface reflectance (pixel values) 24 hours after bruising for hue, saturation, and intensity for three concentric rings both centered and 60 degrees from the bruise center are shown. Ring 1 is the smallest and ring 3 the largest. Ring 3 at 0 degrees and rings 1-3 at 60 degrees represent values for undamaged tissue.

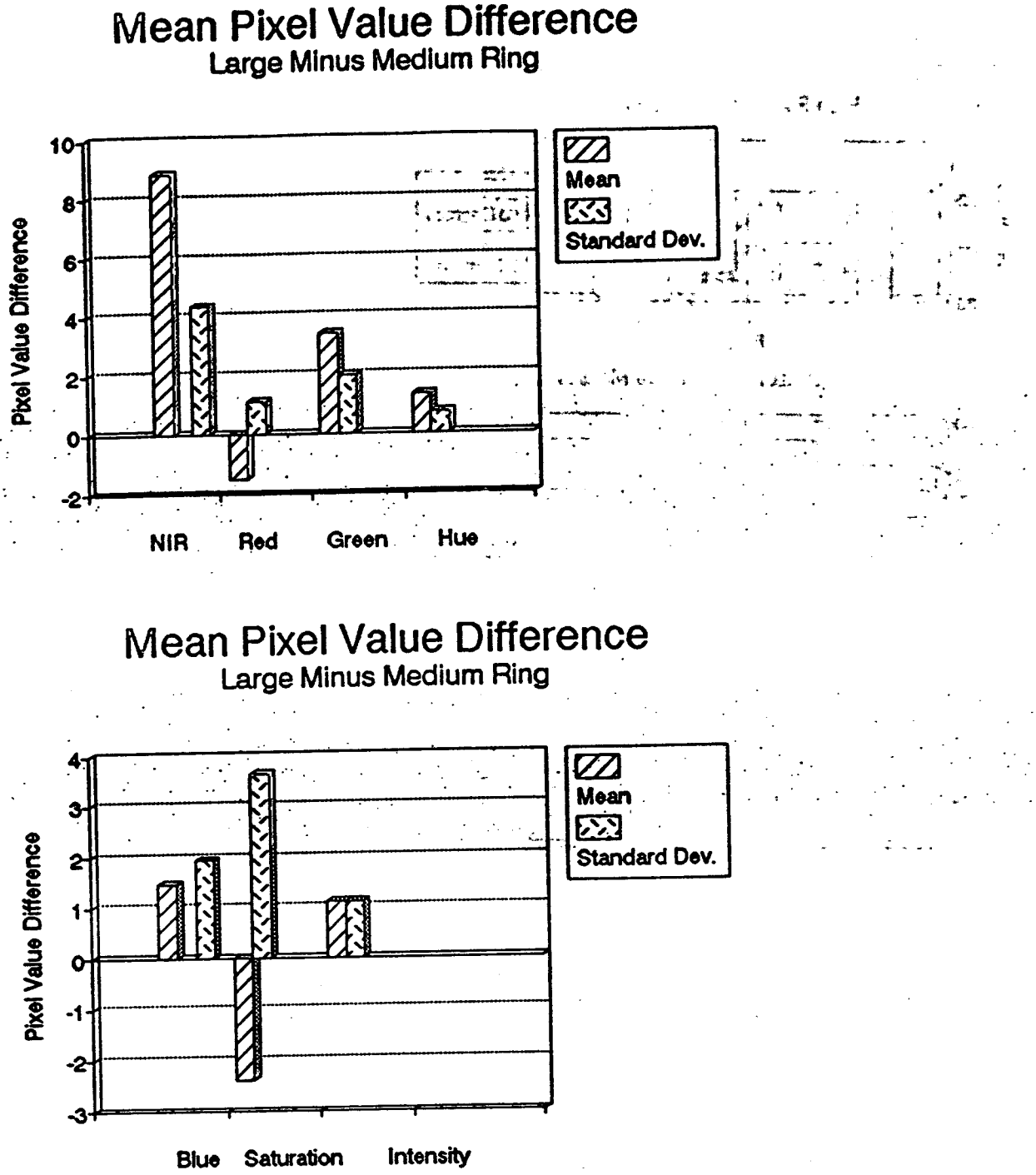

Figure 4. Mean and standard deviations of the difference of pixel values 24 hours after bruising for a medium (bruised) and large (unbruised) ring concentric about the bruise center, with ring diameters equal to the bruise diameter minus 25 pixels and bruise diameter plus 25 pixels, respectively.

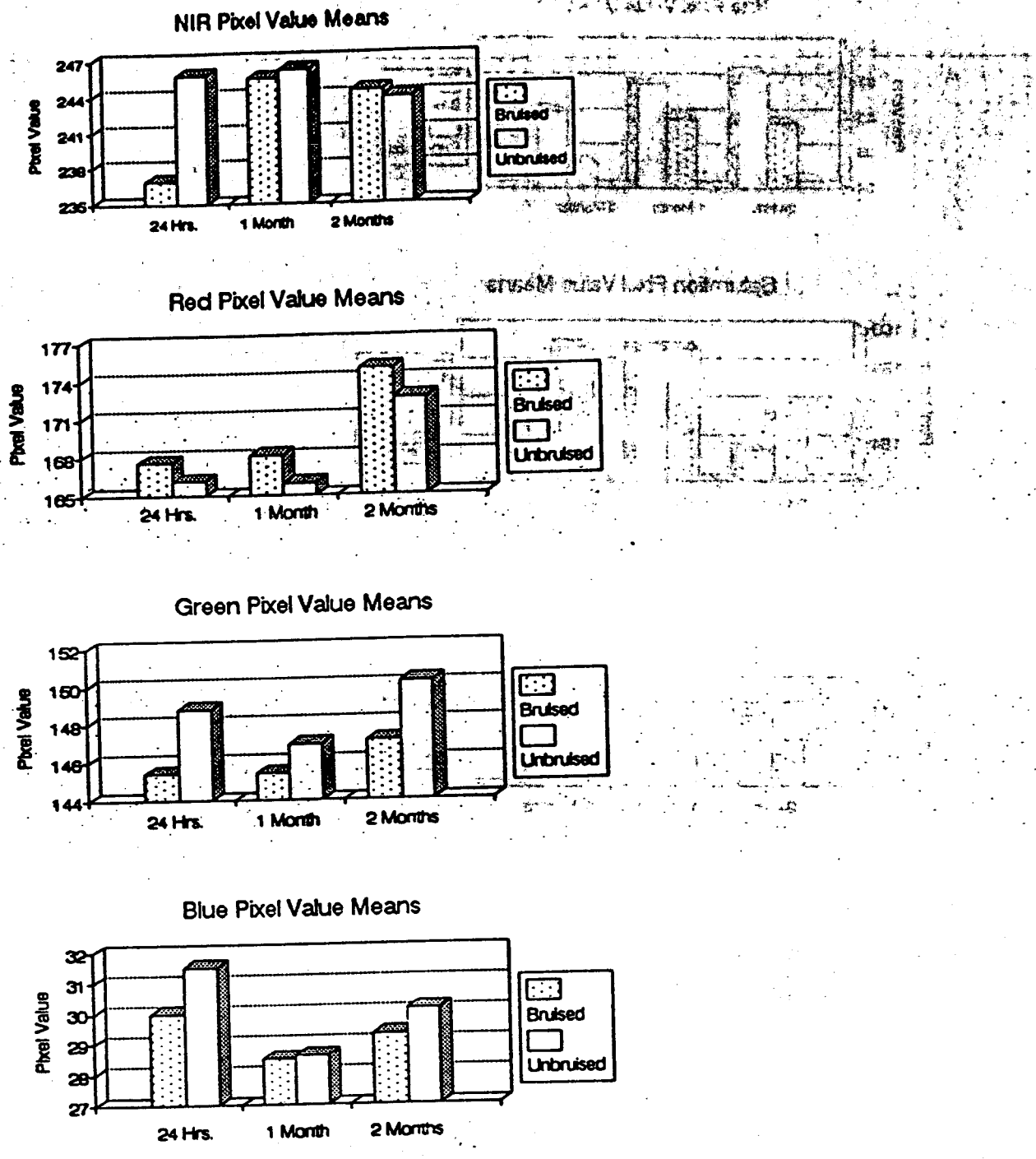

Figure 5. Pixel values representing reflectance at three storage times for NIR, red, green, and blue features using medium (bruised) and large (unbruised) rings concentric about the bruise.

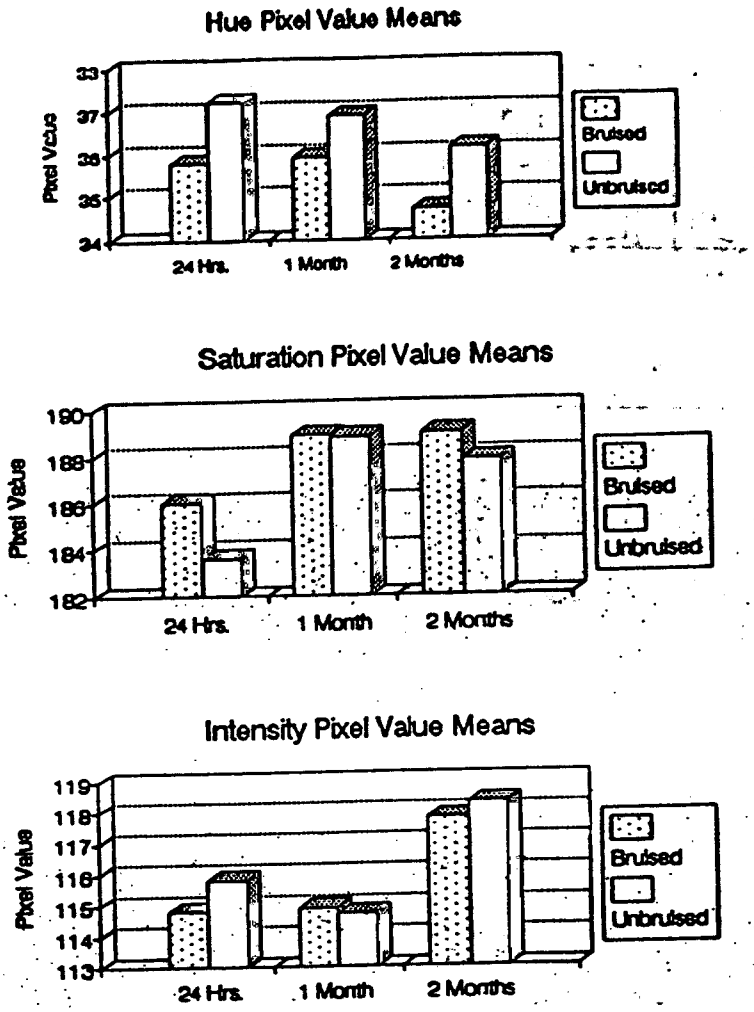

Figure 6. Pixel values representing reflectance at three storage times for hue, saturation, and intensity features using medium (bruised) and large (unbruised) rings concentric about the bruise.

APPENDIX C

Proceedings Optics in Agriculture and Forestry Paper 1836-03
OE/Technology '92

Time effects on near-infrared imaging for detecting bruises on apples

B.L. Upchurch
USDA - ARS
Appalachian Fruit Res. Sta.
45 Wiltshire Rd
Kearneysville, WV 25430

J.A. Throop
Agricultural and Engineering Dept.
Cornell University
Riley-Robb Hall
Ithaca, NY 14853

ABSTRACT

Imaging in the near-infrared region has been used frequently to detect bruises on 'Delicious' apples. Pixel intensities from bruised and nonbruised regions within an image of an apple are compared to characterize the time effects. Near-infrared reflectance from a bruised site is generally lower than the reflectance from a nearby nonbruised region. This difference usually reaches a maximum 24 hours after inducing the bruise. As the bruise ages in storage, reflectance from the bruised region increases. The reflectance continues to increase and eventually exceeds the reflectance from a nonbruised region.

1. INTRODUCTION

Despite a decrease in the number of acres planted, commercial apple production continues to increase. This additional fruit may require automatic handling and harvesting systems. With the use of mechanical systems, there is a higher probability that the fruit will be damaged in the handling process. Therefore, a need exists for an efficient method for detecting and removing damaged fruit.

Since the late 1960's, researchers have tried various techniques for distinguishing bruised from nonbruised apple tissue. There is a decrease in the level of x-ray energy transmitted through bruised apple tissue when compared to nonbruised tissue [5, 16]. Upchurch et al. [13] investigated ultrasonic techniques for distinguishing bruised from nonbruised areas. This technique was based on differences in the acoustic impedance; however, fruit properties such as cuticle and air within the tissues prevented the technique from being successful. Differences between bruised and nonbruised apple tissue were detected with microwave reflectivity, thermal conductivity, conductance, and tissue compressability[7]. However, none of the techniques were successful, because of the wide variability within a single apple and between apples. Danno et al. [3] used thermal imaging to detect temperature differences between damaged and non-damaged regions on apples. When tissue is damaged, a chemical reaction is initiated that results in a temperature increase in the region. This technique was moderately successful when the fruit temperature was closely controlled.

Visible and near-infrared (NIR) reflectance differences between bruised and nonbruised apple tissue has been the most frequently investigated techniques. Freshly bruised apple tissue has a lower reflectance in the visible through near-infrared wavelengths [2, 11]. These earlier observations were expanded by defining specific wavelengths for distinguishing bruised from nonbruised regions on peeled apples [1, 8]. That study was restricted to the wavelength region between 350 and 700 nm. Successful application to nonpeeled apples would be limited by the interference from anthocyanin in the peel. Bruises on unpeeled fruit were detected at wavelengths between 750 and 850 nm [15]. These methods had success but were limited to small inspection areas (19.6 mm^2).

Utilizing advances in computer vision technology and the near-infrared reflectance differences between the two tissue types, a more complex approach was initiated. Digital imaging with statistical pattern recognition located bruises on whole apples by detecting differences in the diffuse reflectance between bruised and nonbruised regions on apples [6]. A line scan camera replaced the matrix camera in order to limit the pixel-to-pixel variation to one dimension [9, 13]. Rehkugler and Throop [9] incorporated machine vision into an automatic sorting system for apples. The design of the apple handling system had a mechanism for orienting and presenting the fruit for inspection by a line scan camera. Based on the thinness-ratio of the binary clusters within an image, apples were sorted into four grades [10]. Attempts to sort apples without orientation on a commercial line were unsuccessful; however, detection of very severe bruises had limited success when apples were placed by hand on a conveyor with the stem-calyx axis perpendicular to the direction of travel [4].

As shown by previous research, automatic bruise detection is a difficult problem caused by the wide variability in reflectance between apples and within a single fruit. Temporal factors have not been formally analyzed. As the bruise ages, the reflectance from that region changes [2, 6]. The objective of this research was to evaluate time effects on the NIR from bruised and nonbruised regions on apples.

2. PROCEDURE

'Delicious' and 'Golden Delicious' apples were hand harvested in mid-September during the 1991 season at the Appalachian Fruit Research Station in Kearneysville, WV. A total of 64 fruit for each variety were placed in tray packs and stored in a cold room at 0°C until needed for testing. Each fruit was bruised by dropping a 39 mm diameter steel disk onto the surface of the fruit 24 hours prior to the first inspection date [15]. Theoretical impact energy was 0.81J. Samples were held at room temperature, 20°C, for 24 hours to allow for bruise development. For each sampling date, fruit were removed from cold storage 24 hours prior to inspection. Fruit were inspected at monthly intervals for three months beginning in November.

Images of apples were acquired and analyzed with an image processing system and solid-state camera. A PC-based system equipped with a Data Translation* frame grabber (DT2851) and frame processor (DT2858) was used to acquire the images. Images were transferred to a VAX 4000/200 (Digital Equipment Corp.) and analyzed with image processing software from Euclid Computer Co. A CCD array camera (Model 4810, COHU Electronics) without the infrared blocking filter was used to acquire images of the apples. A 25mm lens with an aperture set at f1.4 was mounted to the camera. To limit the reflectance from the apple to the NIR region, a long pass filter (Kodak Wratten 89B) was placed between the camera lens and the apple. Two images of each apple were captured. The bruised region was centered in the initial image while a second image was acquired after rotating the apple 135° so that the bruised region was absent in the image. To maintain equivalent measurements between dates, a reference image of a white teflon cylinder was acquired at four times on each date.

The mean value of the pixels around a circular profile at 1° intervals was a measure of the intensity of near-infrared reflectance (NIR) from bruised and

*Mention of a tradename or company does not endorse the use of the products by the United States Government or Cornell University.

nonbruised regions. Three concentric circles were used (Figure 1).

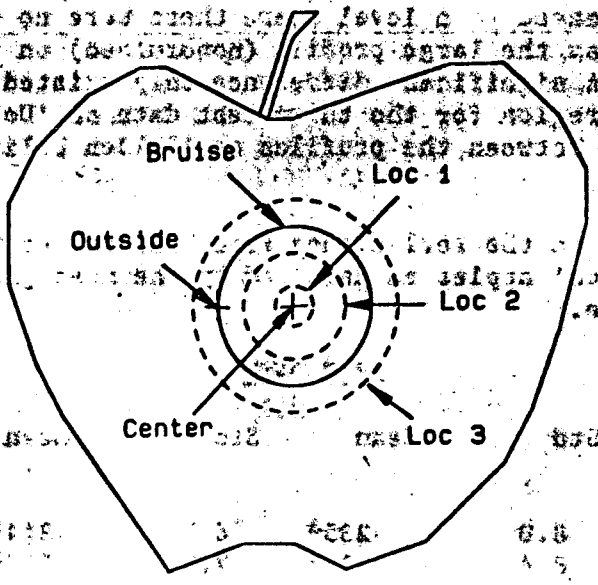

Figure 1. Diagram of apple showing relative size and locations of the circular profiles on the bruised side of the apple. Profiles, sizes and locations were determined by interactively identifying the center and outer diameter of the bruise.

To define the location and size of each circular profile two sites were interactively identified in the image. Initially, the center of the bruised region was interactively identified in the image and used as the center for each concentric profile. Next, the outer edge of the bruised region in the x-direction was identified interactively. The diameter of the middle profile was twice the difference between the center and outer location minus 30 pixels while the outer circle had a diameter twice the difference plus 30. The smallest circular profile had a constant diameter of 10 pixels. After measuring the mean gray value around each circle, the three profiles were applied to the nonbruised side. Each mean value was divided by the mean of the profile for the reference and then multiplied by 255.

3. RESULTS

Time after bruising had a significant effect on the NIR from bruised and nonbruised regions on both 'Delicious' and 'Golden Delicious' apples. Comparing a linear profile that dissected a bruised region, the reflectance from a bruised region decreased to minimum level with time (Figure 2). During one month in storage, the reflectance from the bruised regions increased to a level equivalent to the reflectance from nonbruised regions. This increase in reflectance continued until the reflectance from bruised regions exceeded that from nonbruised regions. Reflectances from 'Golden Delicious' exhibited similar changes with time. For each test date, the significance of each circular profile was tested with a mean separation by SAS GLM contrast (Table 1 and 2). The two profiles from the bruised regions were significantly different ($Pr < 0.05$) from the nonbruised

profiles for the 24 hour test. This difference occurred for both 'Delicious' and 'Golden Delicious' apples. For both varieties, there was no difference between the four nonbruised profiles. After one month in storage, the mean reflectance from bruised regions increased to a level where there were no differences between any profiles, exception was the large profile (nonbruised) on the bruised side for the 'Golden Delicious'. A significant difference only existed for the middle profile from the bruised region for the third test date on 'Delicious'. However, there were no differences between the profiles on 'Golden Delicious' for the final date.

Table 1. Effects of time on the reflectance from bruised and nonbruised regions on 'Red Delicious' apples as measured by the mean gray-level of a circular profile.

Profile Size	TEST DATE Nov Mean	Nov Std	Dec Mean	Dec Std	Jan Mean	Jan Std
BRUISED SIDE						
small	231[a]	8.0	235[a]	6.5	244[a]	4.1
medium	230[a]	8.4	235[a]	7.3	247[b]	3.8
large	241[b]	7.6	238[a]	5.0	242[a]	3.7
NONBRUISED SIDE						
small	244[b]	7.5	242[a]	5.0	244[a]	4.9
medium	243[b]	7.5	241[a]	5.1	244[a]	4.5
large	242[b]	7.5	239[a]	4.8	243[a]	4.4

*Means with the same letter are not significantly different at the 95% confidence level.

Table 2. Effects of time on the reflectance from bruised and nonbruised regions on 'Golden Delicious' apples as measured by the mean gray-level of a circular profile.

Profile Size	TEST DATE Nov Mean	Nov Std	Dec Mean	Dec Std	Jan Mean	Jan Std
BRUISED SIDE						
small	238[c]	8.0	244[b]	6.5	244[a]	4.1
medium	237[c]	8.4	246[a]	7.3	244[a]	3.8
large	246[ab]	7.6	246[a]	5.0	244[a]	3.7
NONBRUISED SIDE						
small	247[a]	7.5	244[b]	5.0	243[a]	4.9
medium	246[ab]	7.5	244[b]	5.1	242[a]	4.5
large	249[b]	7.5	245[a]	4.8	243[a]	4.4

*Means with the same letter are not significantly different at the 95% confidence level.

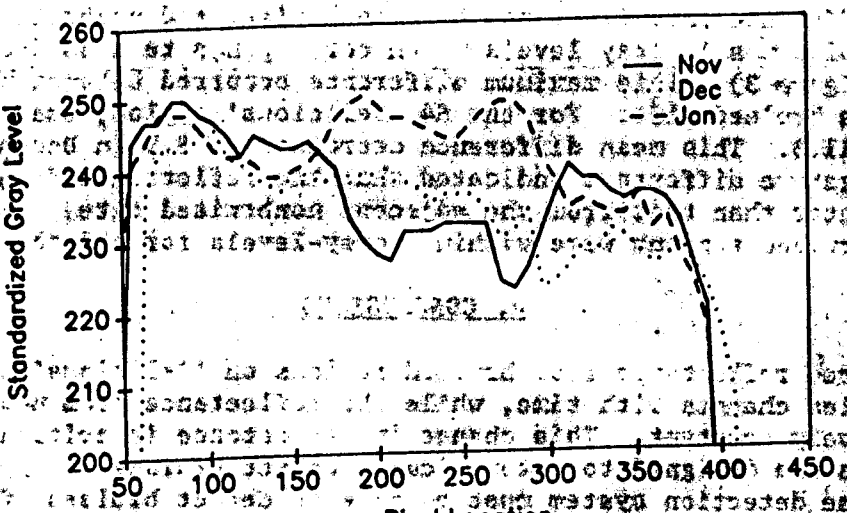

Figure 2. Typical pixel intensities across a bruised section on an apple. Each point in the linear profiles was the average of six adjacent pixels.

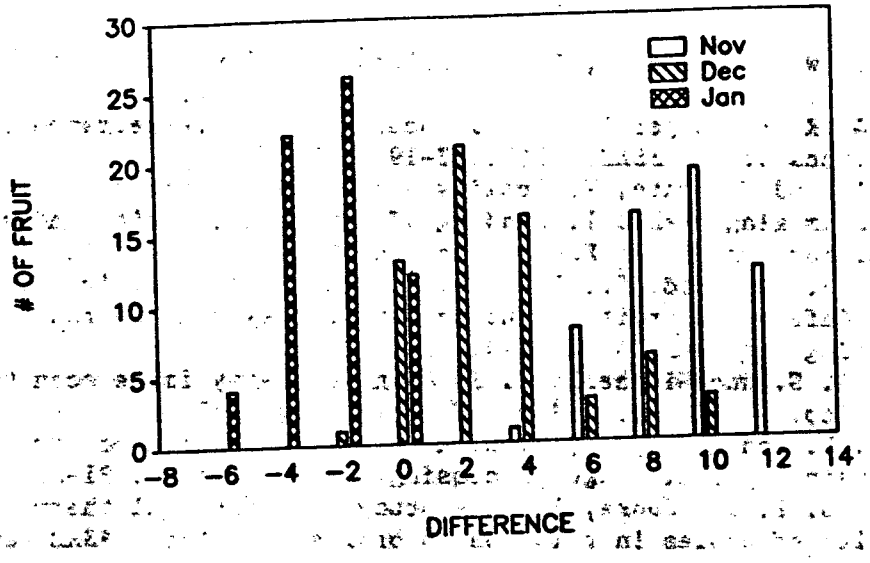

Figure 3. Distribution of the differences between the larger two profiles on the bruised side of the fruit. A negative difference indicated that the reflectance from the bruised region was greater than that from the adjacent nonbruised site.

Automatic bruise detection by machine vision depends upon the ability of the system to detect spatial and magnitude relationships between groups of pixels. The maximum difference in reflectance between bruised and nonbruised areas on 'Delicious' apples was 12 gray levels which corresponds to a 5% decrease in reflectance (Figure 3). This maximum difference occurred between the larger two profiles on the bruised side. For the 64 'Delicious' apples, the mean difference was initially 11.3. This mean difference decreased to 3.5 in December and -4.5 in January. A negative difference indicated that the reflectance from the bruised region was greater than that from the adjacent nonbruised site. Mean differences among the nonbruised regions were within 2 gray-levels for all three test dates.

4. CONCLUSIONS

Near-infrared reflectance from bruised regions on 'Delicious' and 'Golden Delicious' apples changes with time, while the reflectance from nonbruised regions remains relatively constant. This change in reflectance is critical when machine visions systems are designed to automatically detect bruises on apples. An automatic bruise detection system must be able to detect bruises of various age. However, the task is more complicated by the fact that the amount of light reflected from the bruised area varies with time.

5. ACKNOWLEDGEMENT

This research supported by a Grant No. US-1573-88R from BARD, The United States-Israel Binational Agricultural Research and Development Fund.

6. REFERENCES

1. Bilanski, W. K. and Penn, C. L. Bruise detection using optical reflectance parameters. Canadian Agric. Engng., 26(2):111-114, 1984.
2. Brown, G. K. and Segerlind, L. J. Near-infrared reflectance of bruised apples. Transactions of the ASAE, 17(1):17-19, 1974.
3. Danno, A. and Miyazato, M. Quality evaluation of agricultural products by infrared imaging method I: Grading of fruits for bruise and other surface defects. Memoirs of the Fac. Agric. 14(23):123-138, 1978.
4. Davenel, A., Guizard, C., Labarre, T., and Sevila, F. Automatic detection of surface defects on fruits by using a vision system. Journal of Agricultural Engineering Research, 41(1):1-9, 1988.
5. Diener, R. G. and Mitchell, J. P. Using an X-ray image scan to sort bruised apples. Rep. J-380. Amer. Soc. of Agric. Eng. 1970.
6. Graf, G. L. and Rehkugler, G. E. Automatic detection of surface flaws on apples using digital image processing. ASAE Paper No. 81-3537, 1981.
7. Holcomb, D. P. and Cooke, J. R. A study of electrical thermal and mechanical properties of apples in relation to bruise detection. ASAE Paper No. 77-3512, 1977.
8. Pen, C.L., Bilanski, C. W., and Fuzzen, D.R. Classification analysis of good and bruised apple tissue using the measured optical reflectance. Transactions of the ASAE, 18(1)326-330, 1985.
9. Rehkugler, G. E. and Throop, J. A. Apple sorting with machine vision. Transactions of the ASAE, 29(5):1388-1397, 1986.
10. Rehkugler, G. E. and Throop, J. A. Image processing algorithm for apple defect detection. ASAE Paper No. 87-3041, ASAE, St. Joseph, MI 49085, 1987.

11. Reid, W. S. Optical detection of apple skin, bruise, flesh, stem, and calyx. Journal of Agric. Engng. Res., 21(3):291-295, 1976.
12. SAS. SAS/STAT Guide. ver 6, SAS Institute, Inc., Box 8000, Cory, NC 27517.
13. Taylor, R. W. and Rehkugler, G. E. Apple bruise detection. Agricultural Electronics - 1983 and Beyond, Vol. II, ASAE, St. Joseph, MI 49085, 652-662, 1984.
14. Upchurch, B. L., Miles, G. E., Stroshine, R. L. Furgason, E. S. and Emerson, F. H. Ultrasonic measurement for detecting apple bruises. Transactions of the ASAE. 30(3):803-809, 1987.
15. Upchurch, B. L., Affeldt, H. A., Hruschka, W. R., Norris, K. H. and Throop, J. A. Spectrophometric study of bruises on whole 'Red Delicious' apples. Transactions of the ASAE 33(2):585-589, 1990.
16. Ziegler, G. E. and Morrow, C. T. Radiographic Bruise Detection, ASAE Paper No. 70-533, 1970.